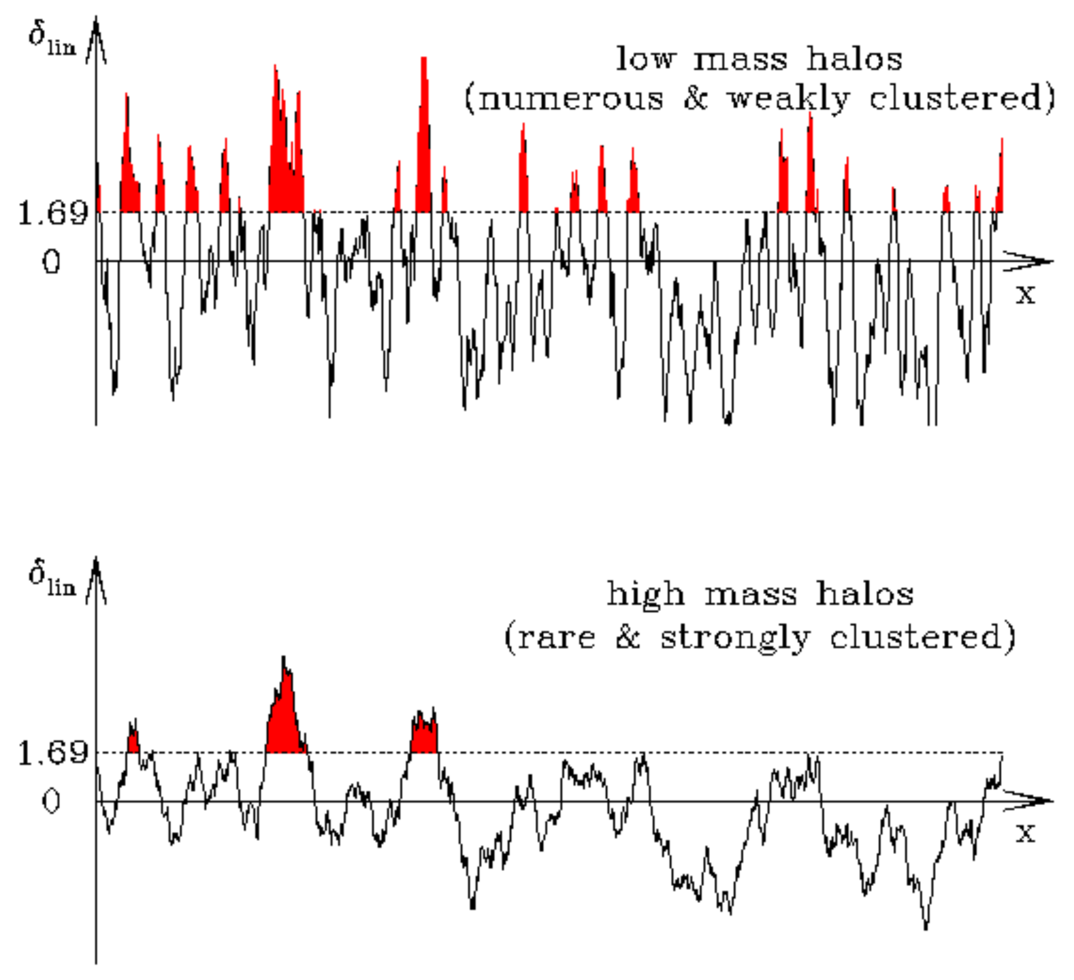

Expect that the brightest, or the most massive, objects at any cosmic epoch represent an "amplified" version of the dark matter distribution

(e.g., galaxy clusters clump with one another more strongly than typical galaxies do)

GALAXY FORMATION: High Peaks in the Matter Distribution

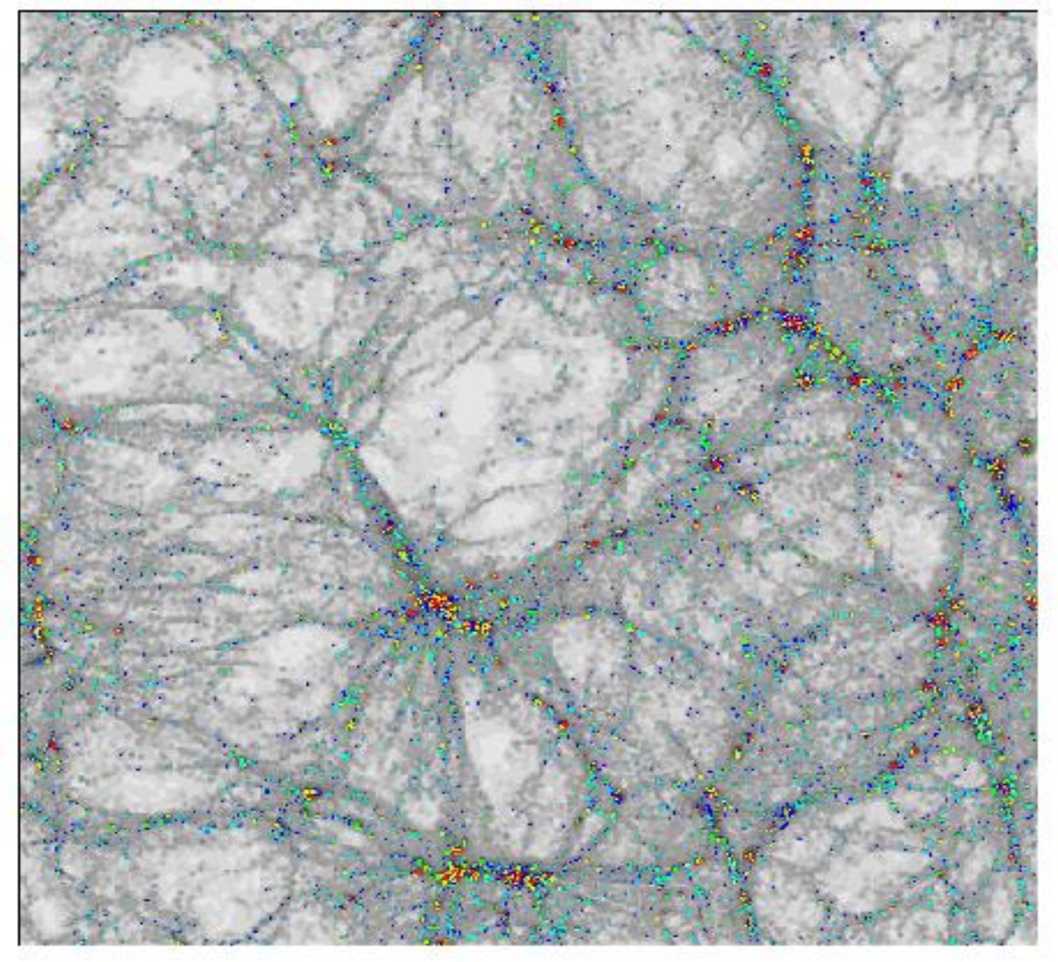

Virgo consortium, 1999

Galaxies here are color-coded according to the cosmic epoch of their original collapse-- red galaxies are the oldest, **blue** the youngest.

Galaxies in the most strongly clustered regions formed first.

Decent qualitative match to the observed universe.

SFR density vs. Redshift

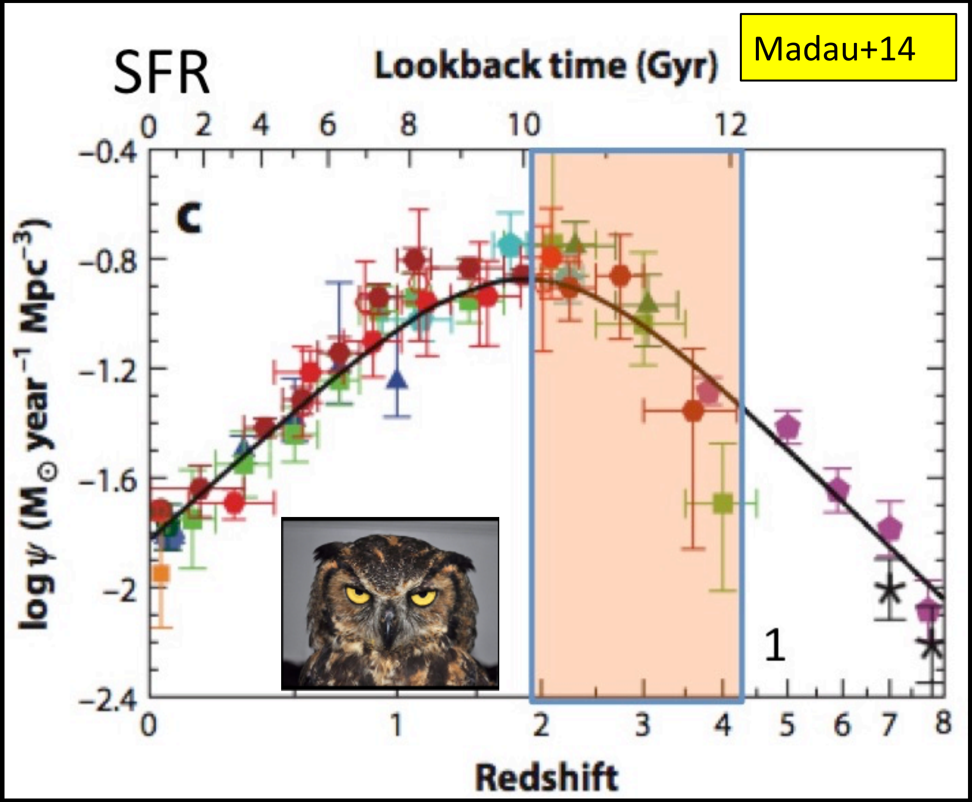

sSFR = (SFR/M*) vs Redshift

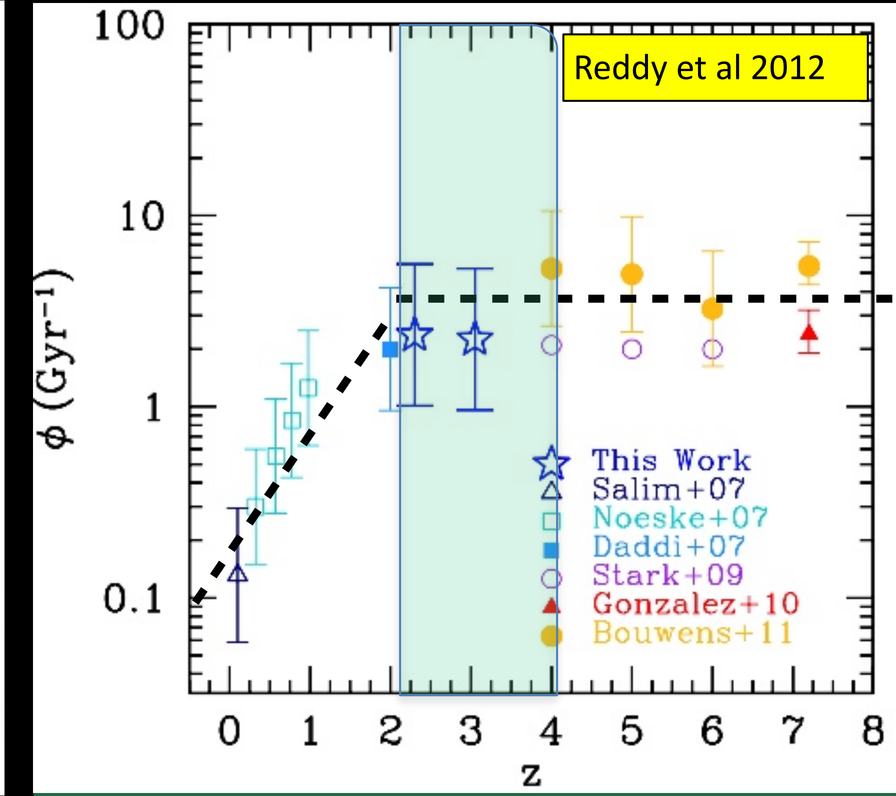

$$\frac{1}{M^*}\frac{dM^*}{dt} = \text{sSFR} \approx 4-5\ \text{Gyr}^{-1} \sim \frac{1}{\tau} \quad ; \quad \tau \sim 200\ \text{Myr}$$

e-folding time for increase
in SFR for individual galaxies

Star Formation/Black Hole Accretion History of the Universe

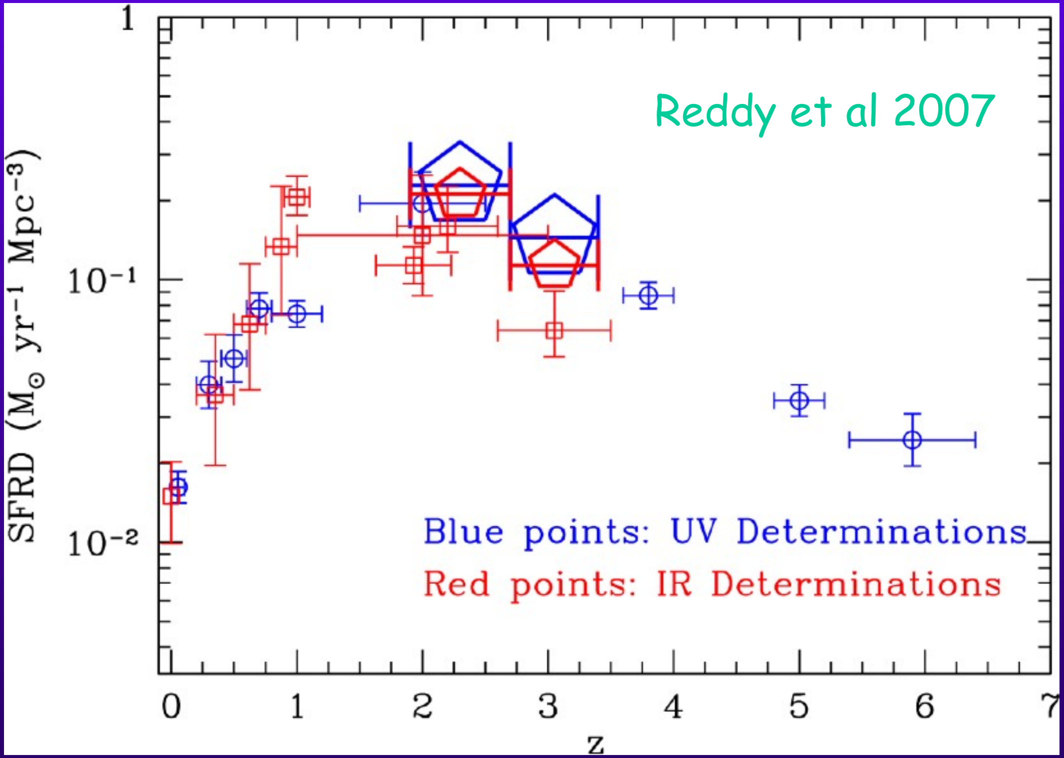

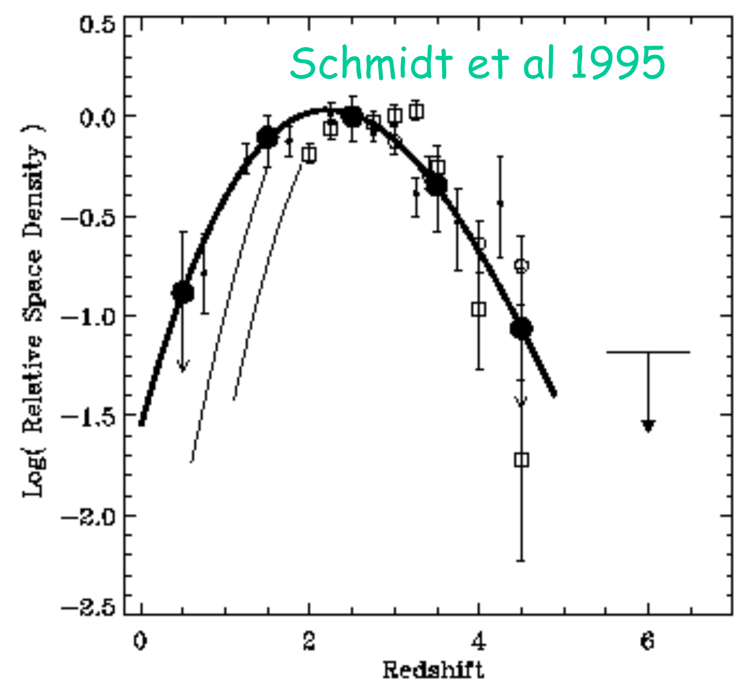

Galaxies

Bright Quasars

Tracing the "Cosmic Web" with Diffuse Gas

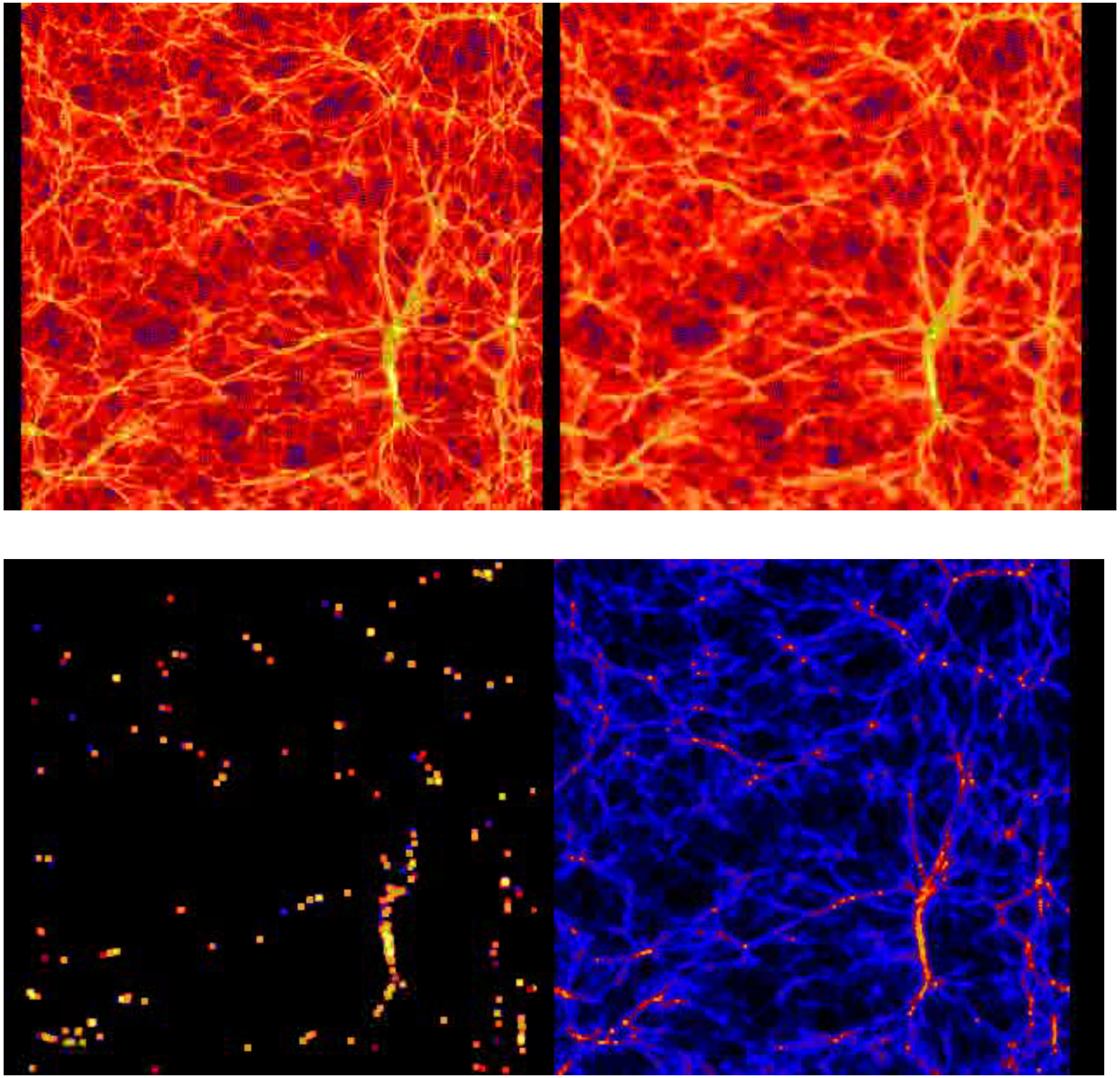

Quasar Absorption Lines

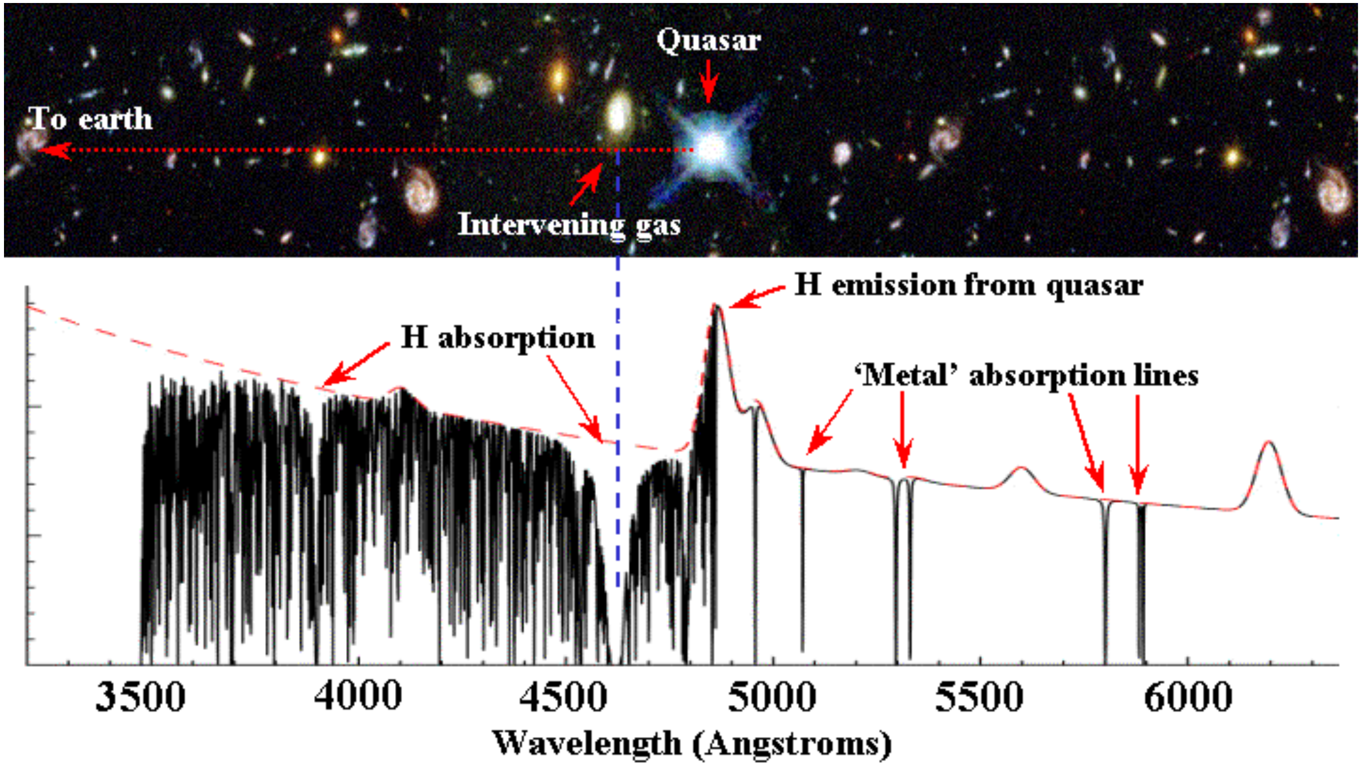

- use quasars as bright "beacons" for probing intervening gaseous material
- can study both galaxies and diffuse gas that produces no luminosity at any wavelength

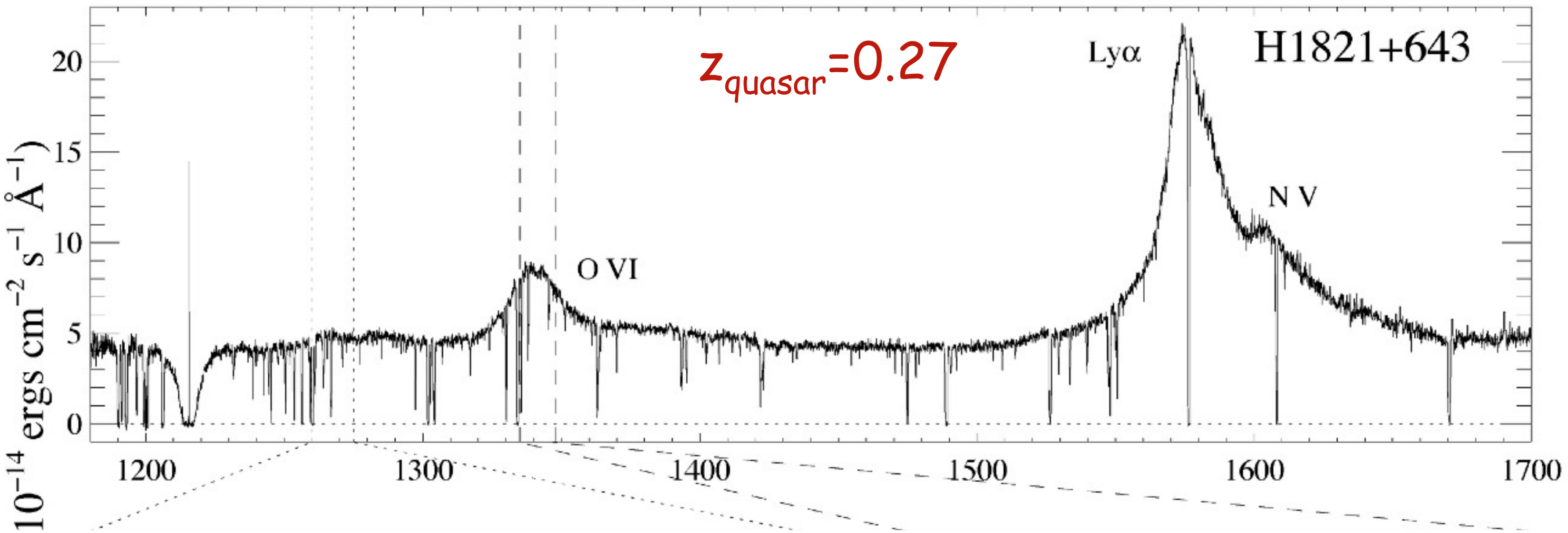

z_{quasar}=0.27

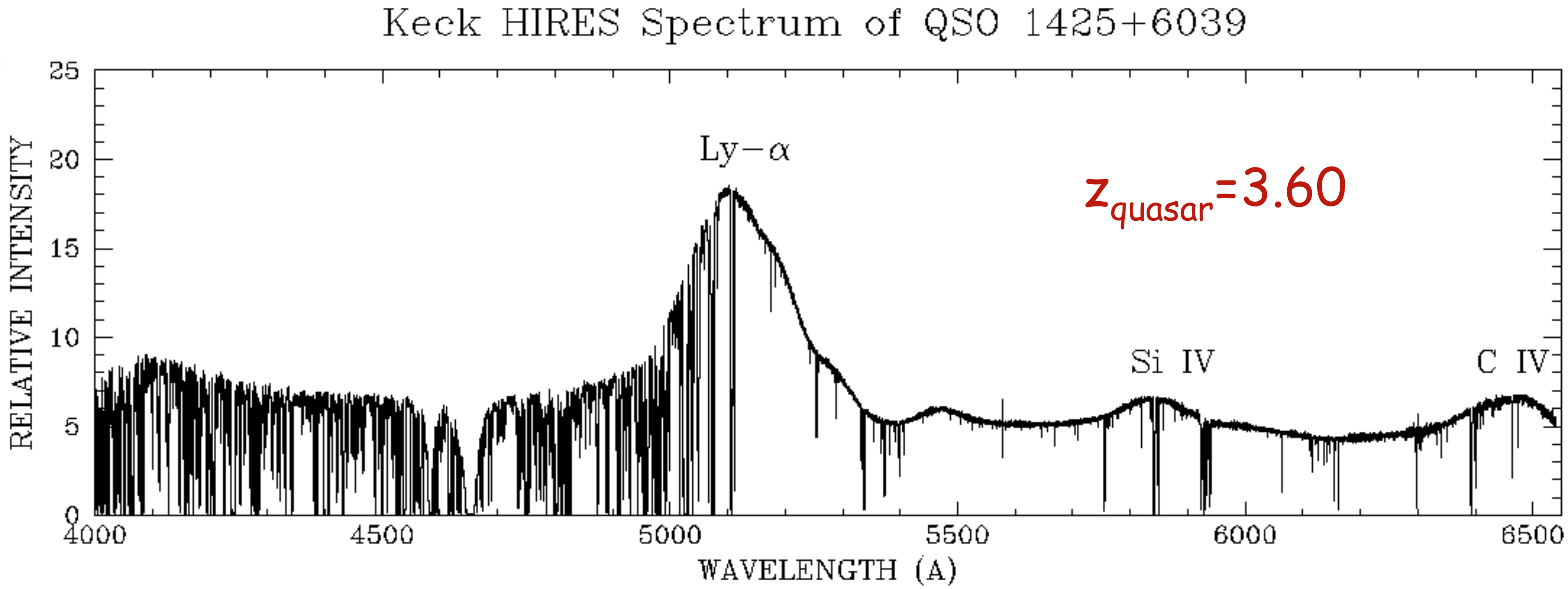
Keck HIRES Spectrum of QSO 1425+6039

z_{quasar}=3.60

$\lambda_{obs(Ly\alpha)} = (1+z_{cloud}) \times 1216$ Angstroms

The “Lyman Alpha Forest” of Neutral Hydrogen

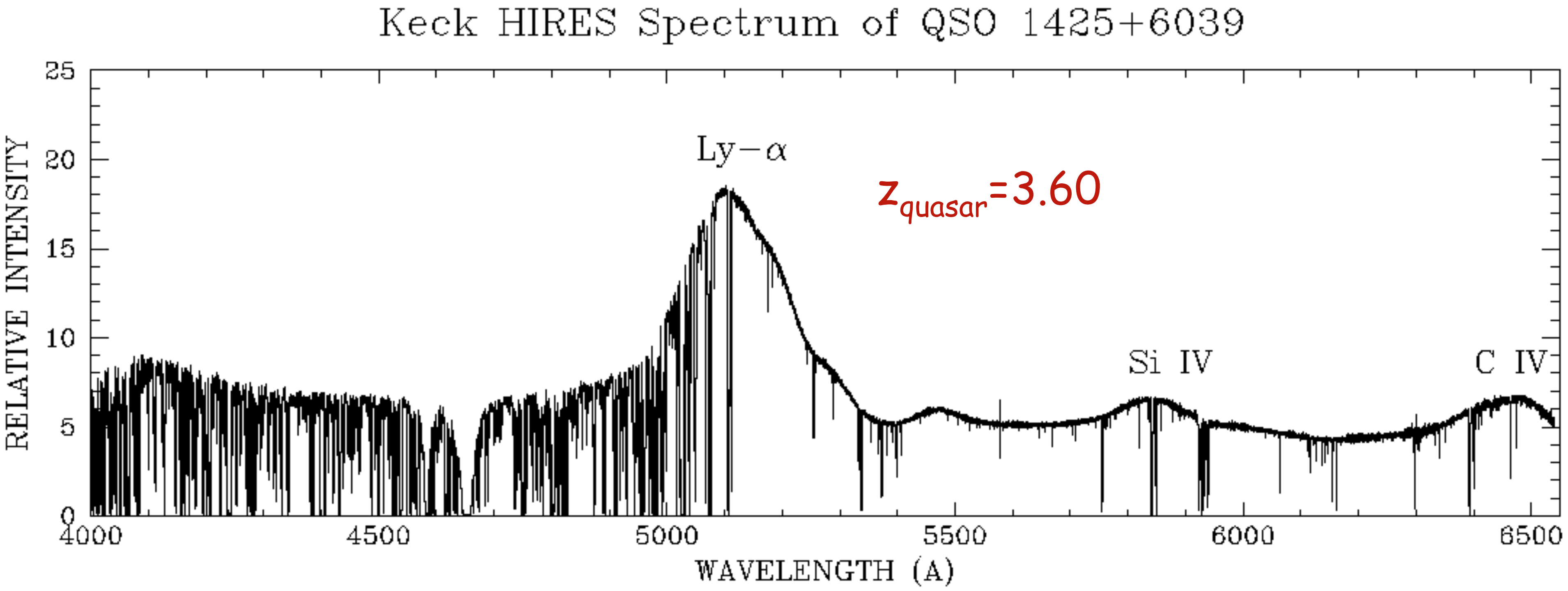

$\lambda_{obs}=(1+z_{cloud})\times1216$ Angstroms

High-resolution Quasar Spectrum, z_Q=2.720

$\lambda_{obs} = \lambda_{rest}(1+z)$

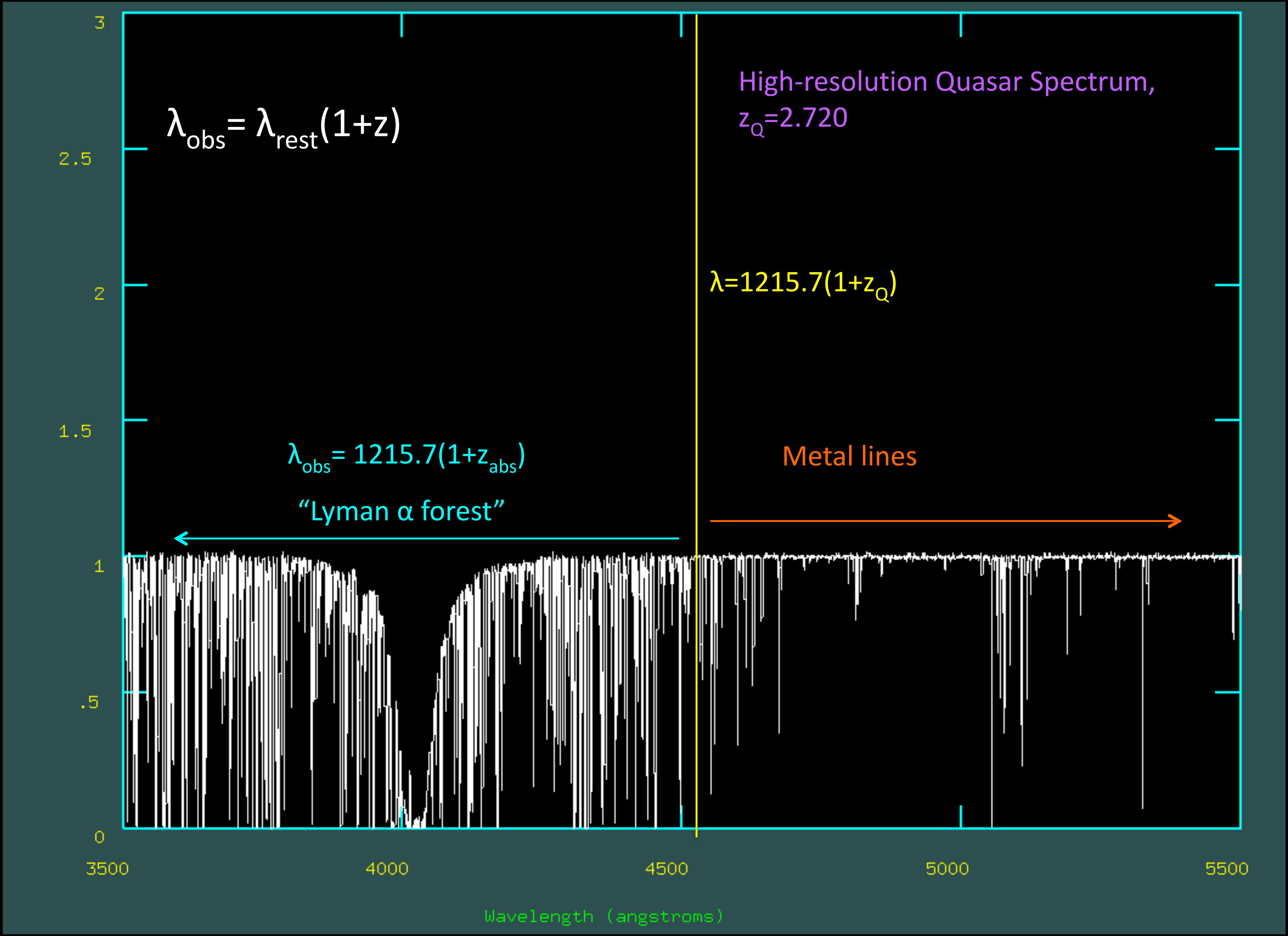

$\lambda = 1215.7(1+z_Q)$

$\lambda_{obs} = 1215.7(1+z_{abs})$

"Lyman α forest"

Metal lines

Why z=2-3 is Optimal for Establishing Statistical Baselines for High Redshift Galaxies

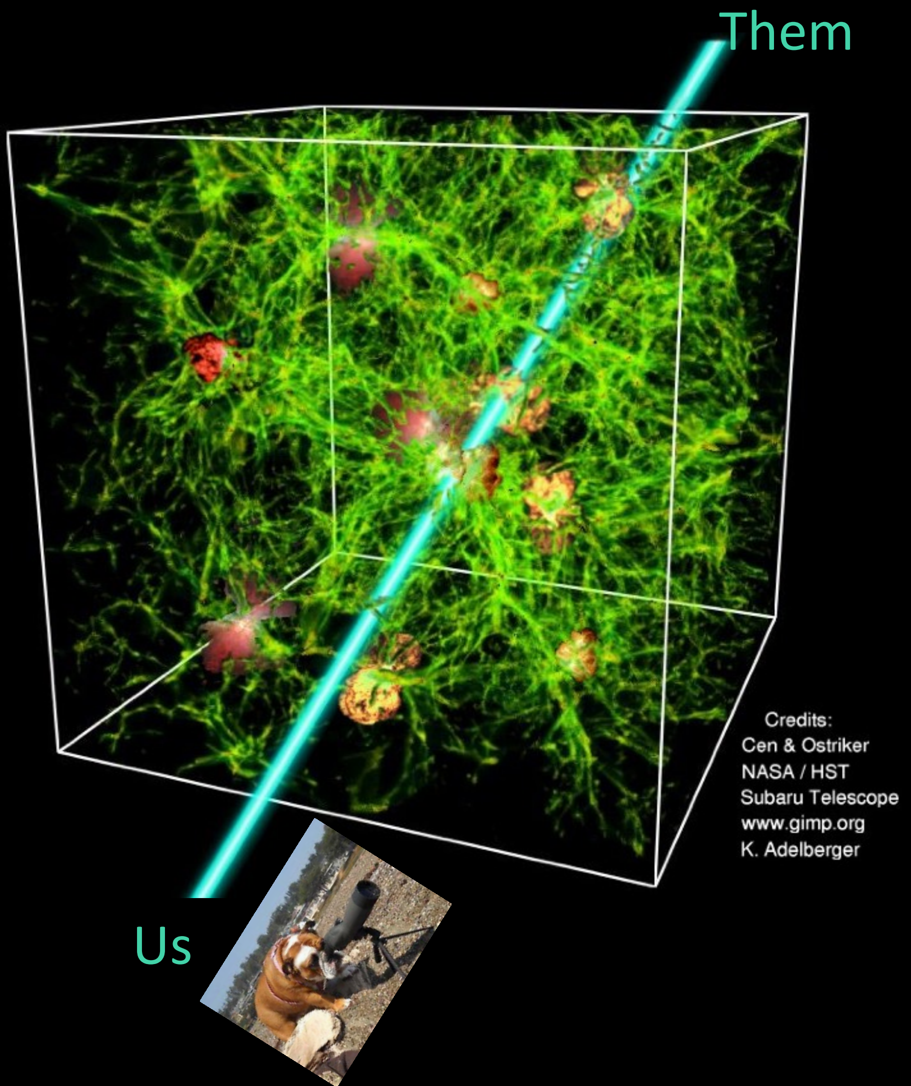

Credits:
Cen & Ostriker
NASA / HST
Subaru Telescope
www.gimp.org
K. Adelberger

At z~2-3, IGM remains "porous" enough to study baryons outside of galaxies

→ CGM, IGM

Value added by having access to diffuse gas in absorption is HUGE

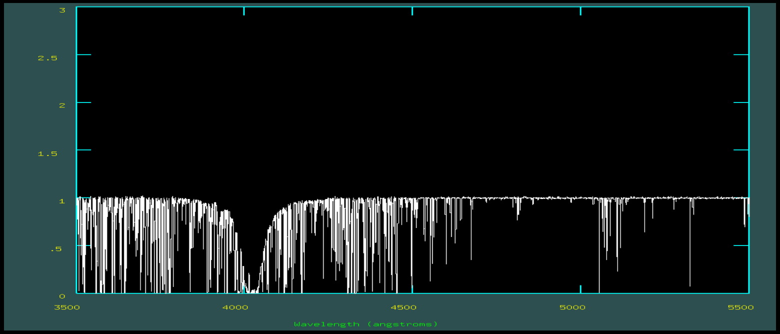

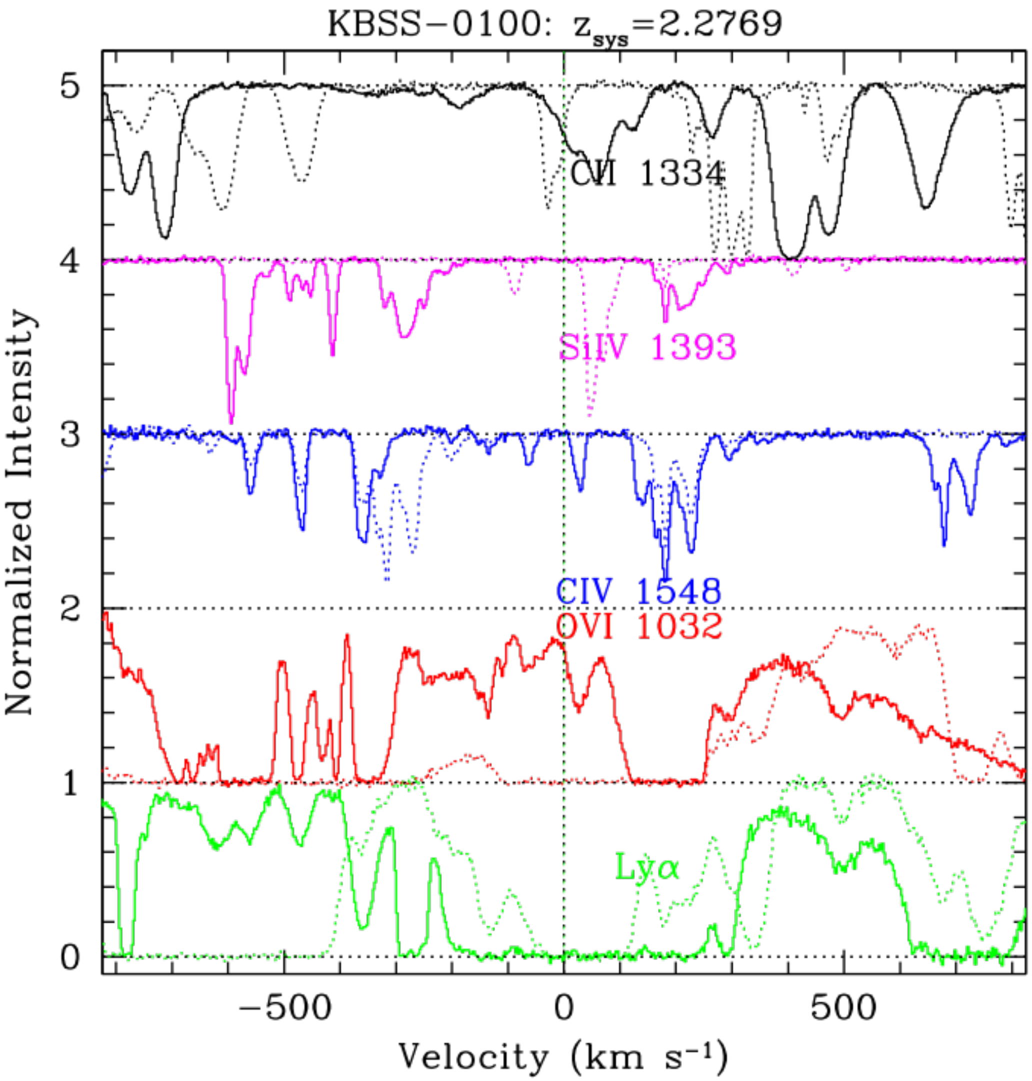
KBSS−0100: z_{sys}=2.2769
Normalized Intensity
5
4
3
2
1
0
CII 1334
SiIV 1393
CIV 1548
OVI 1032
Lyα
−500
0
500
Velocity (km s⁻¹)

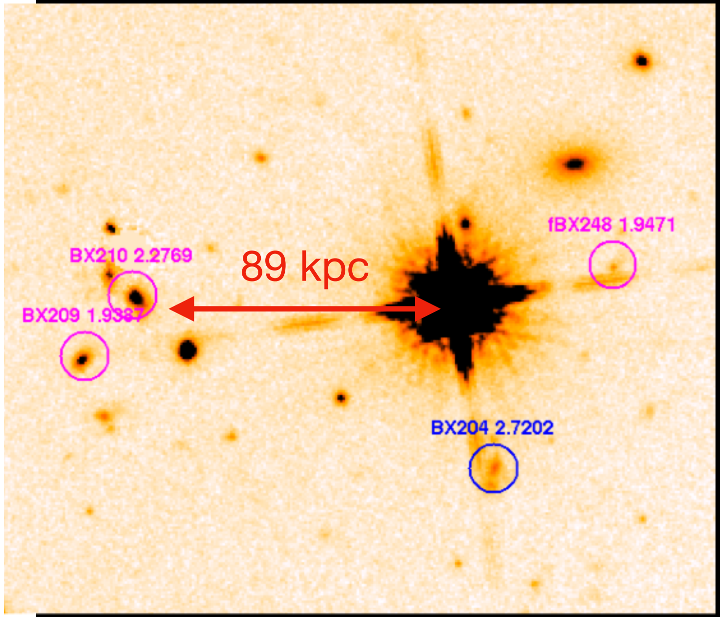
BX210 2.2769
BX209 1.9387
fBX248 1.9471
BX204 2.7202
89 kpc

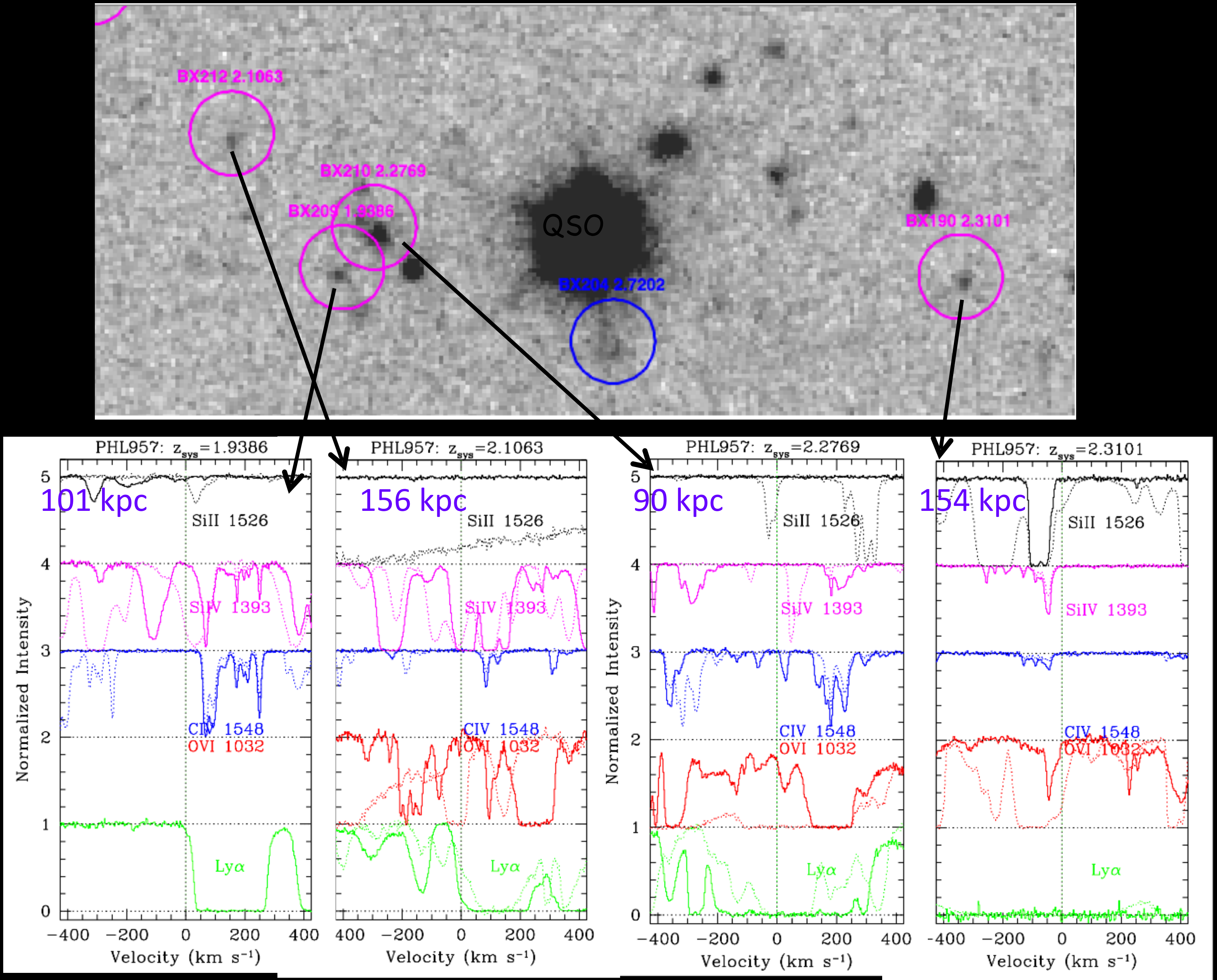
BX212 2.1063
BX210 2.2769
BX209 1.9886
QSO
BX204 2.7202
BX190 2.3101
PHL957: z_{sys}=1.9386
101 kpc
PHL957: z_{sys}=2.1063
156 kpc
PHL957: z_{sys}=2.2769
90 kpc
PHL957: z_{sys}=2.3101
154 kpc
SiII 1526
SiIV 1393
CIV 1548
OVI 1032
Lyα
Normalized Intensity
0
1
2
3
4
5
−400
−200
0
200
400
Velocity (km s⁻¹)

Near Solar Metallicity at Δv~+200 km/s

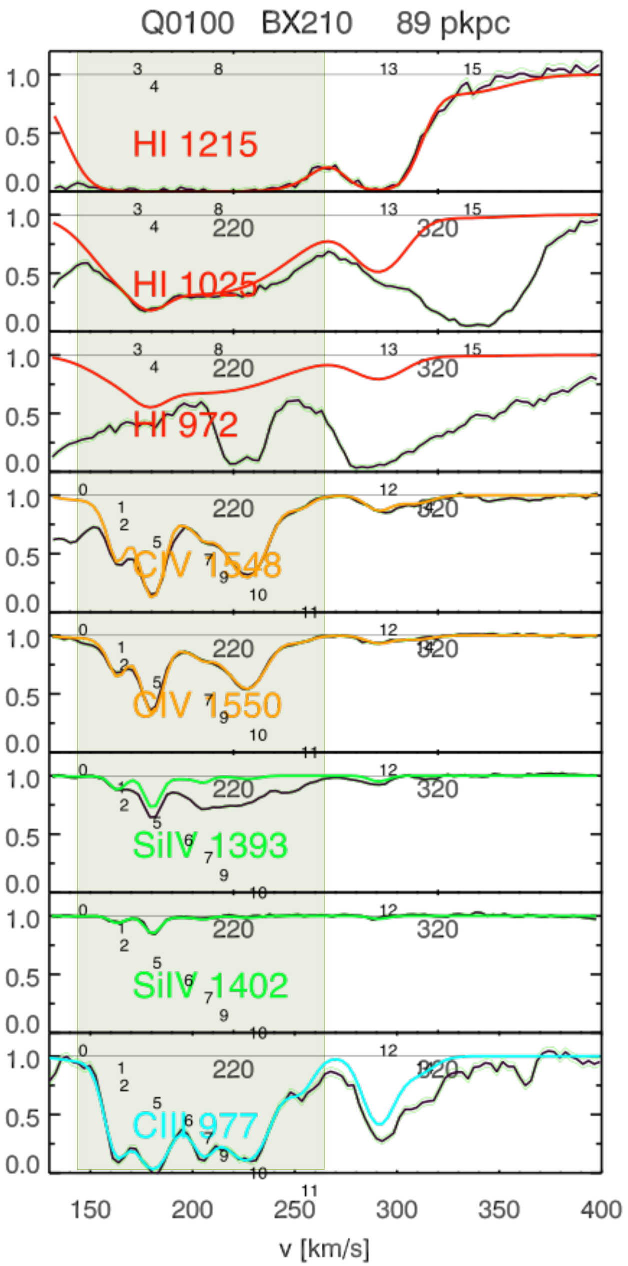

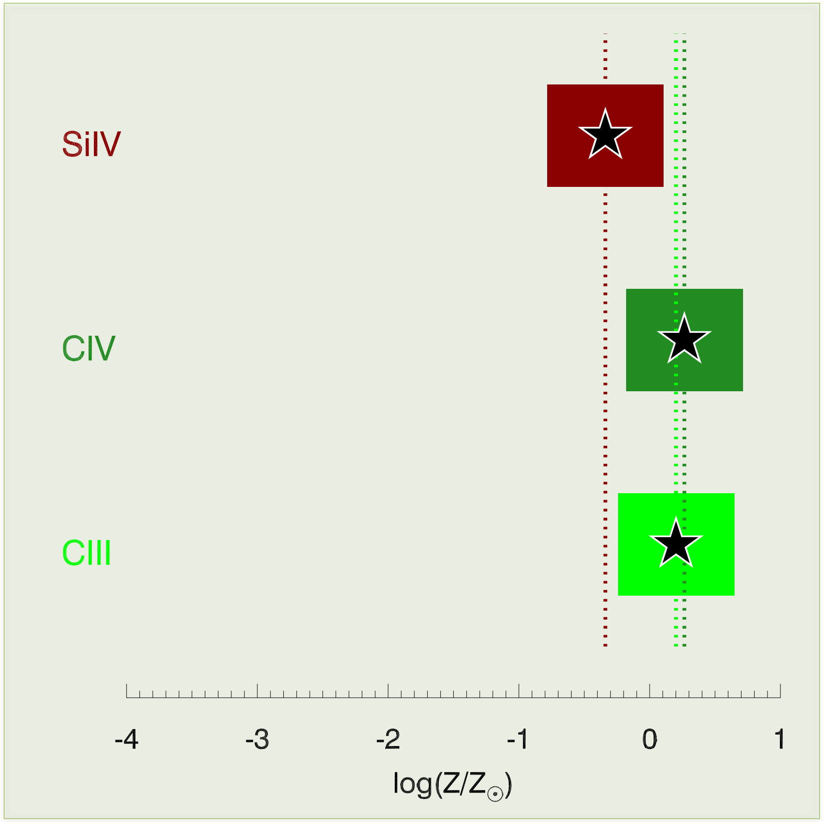

Rudie + in prep

BX182: D_{gal}=75 kpc, z=2.3555

Path separation=0.4 kpc

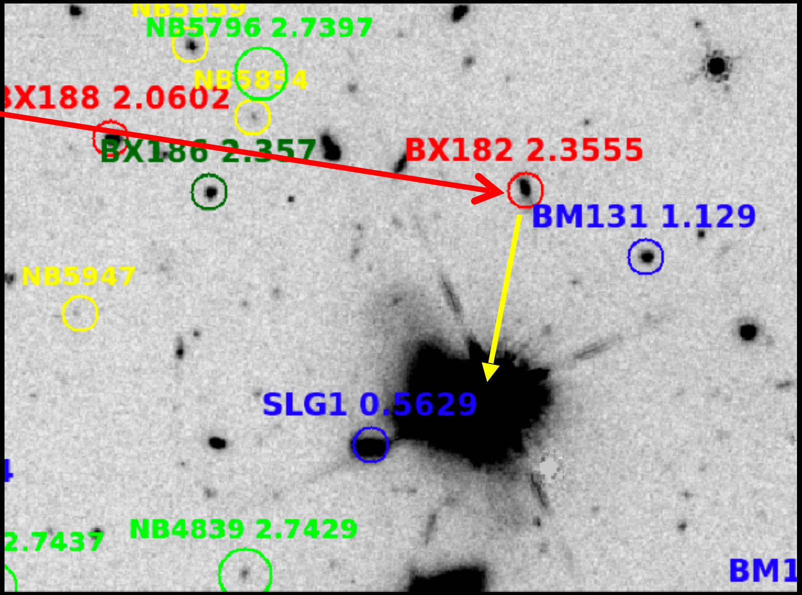

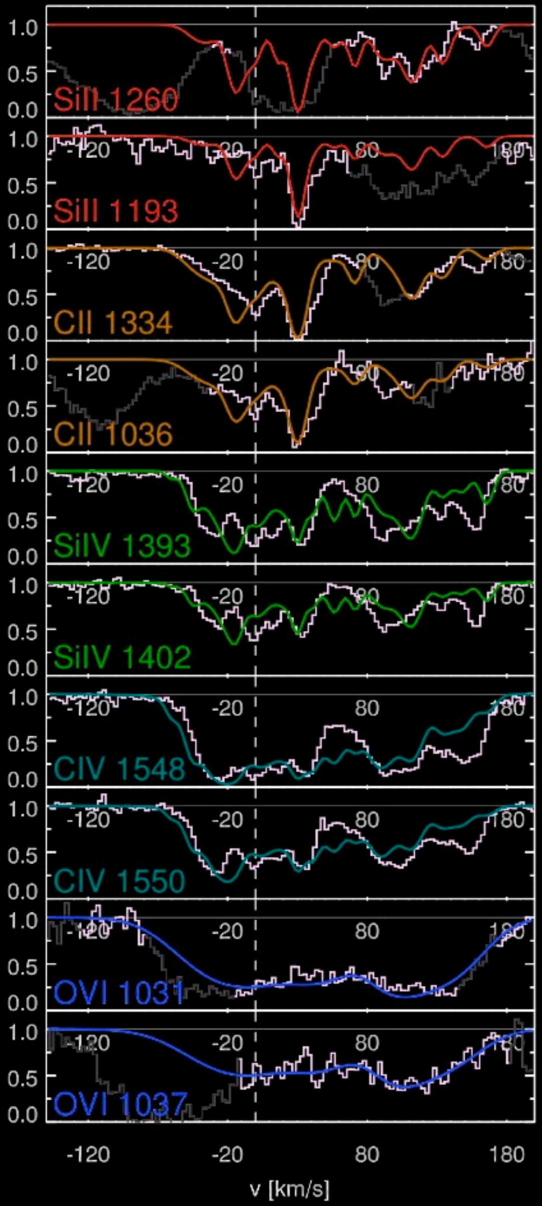

Rudie, CS,+2019

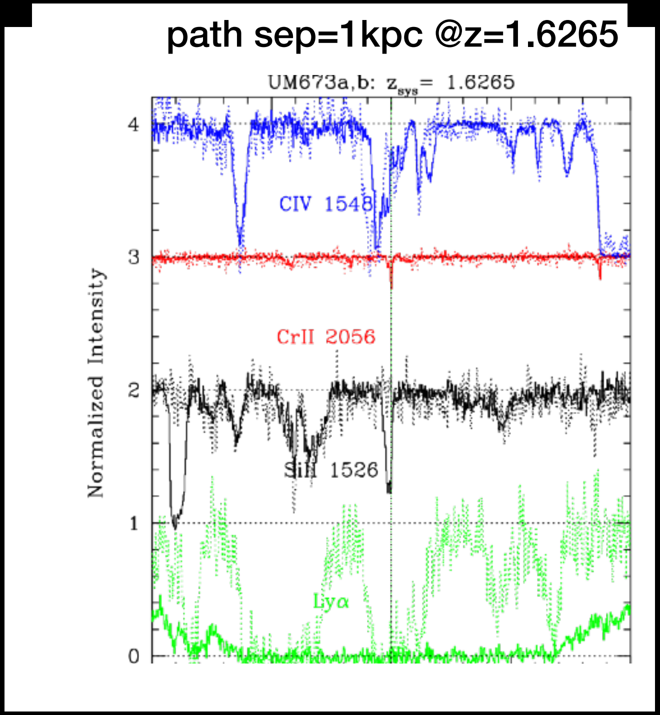
path sep=1kpc @z=1.6265

Cooke, Pettini, C.S.+2010

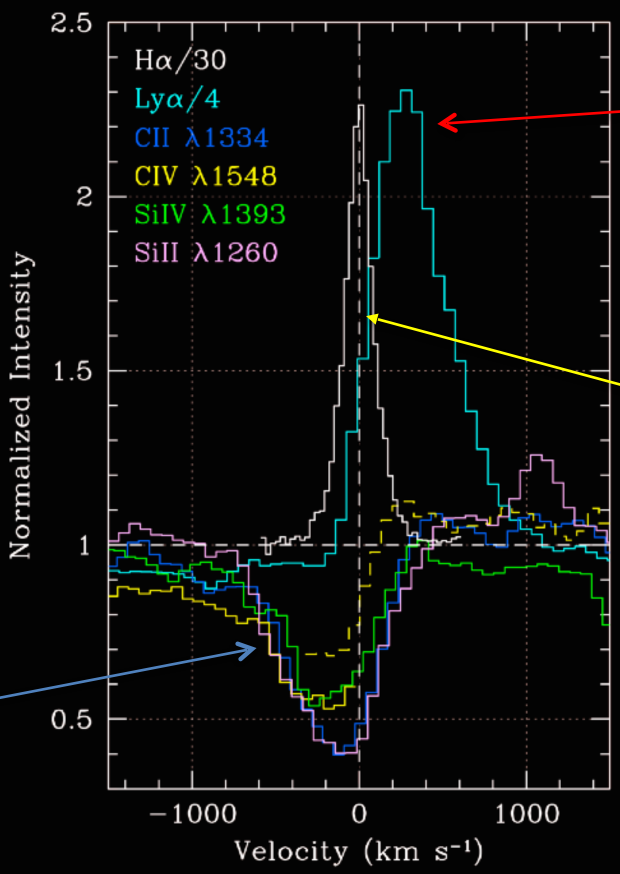

Resonance Lyman α photons scattered from “back” side of flow- acquire redshift with respect to stars

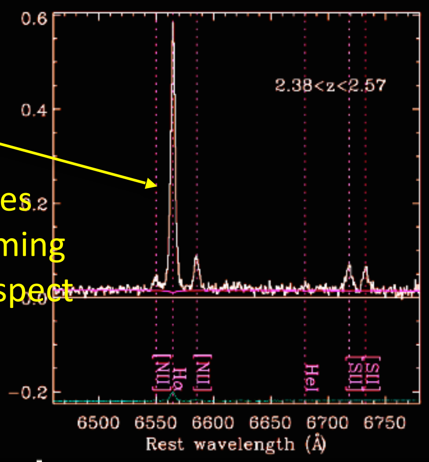

Nebular emission lines from gas around forming stars- at rest with respect to galaxy redshift

Photons absorbed by gas moving toward observer, acquire blueshift

astronomer

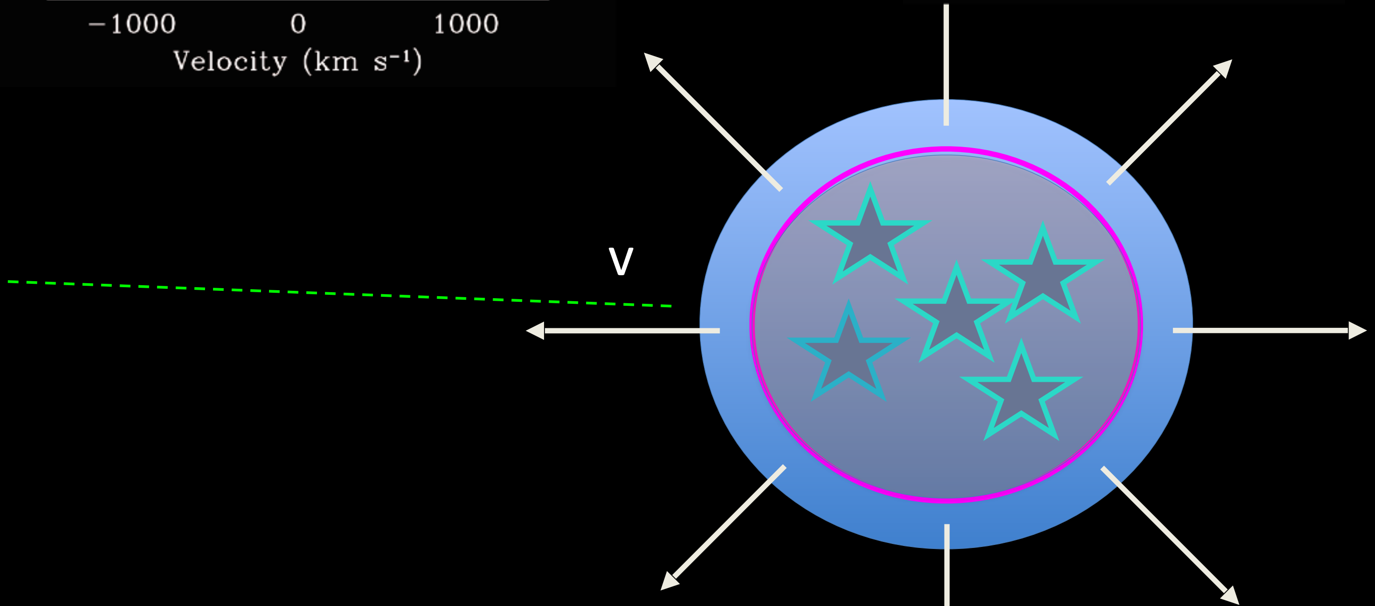

Down the Barrel (Slit Spectrum)

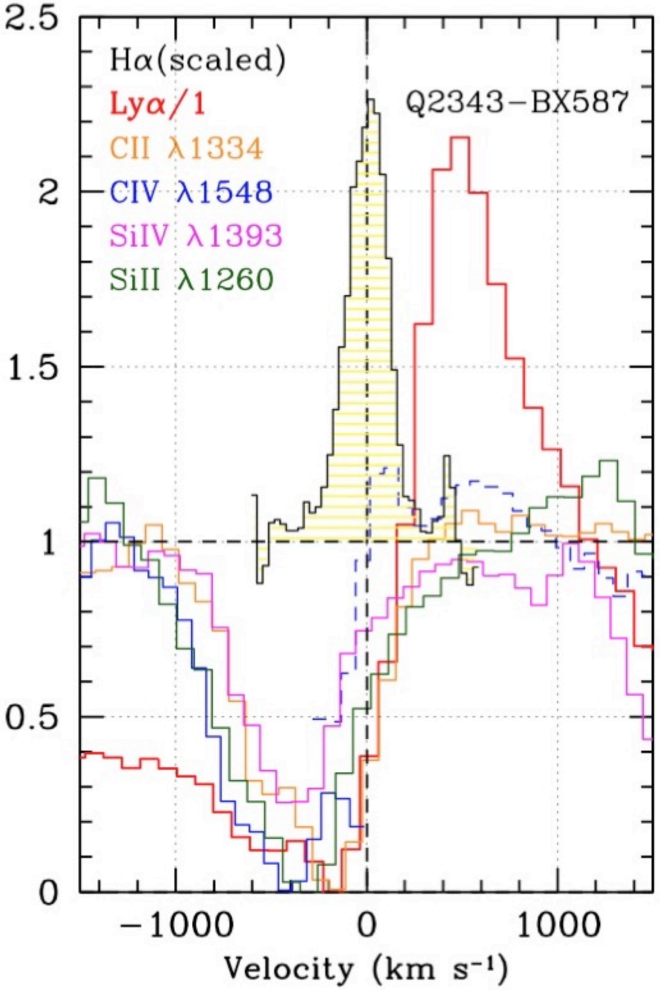

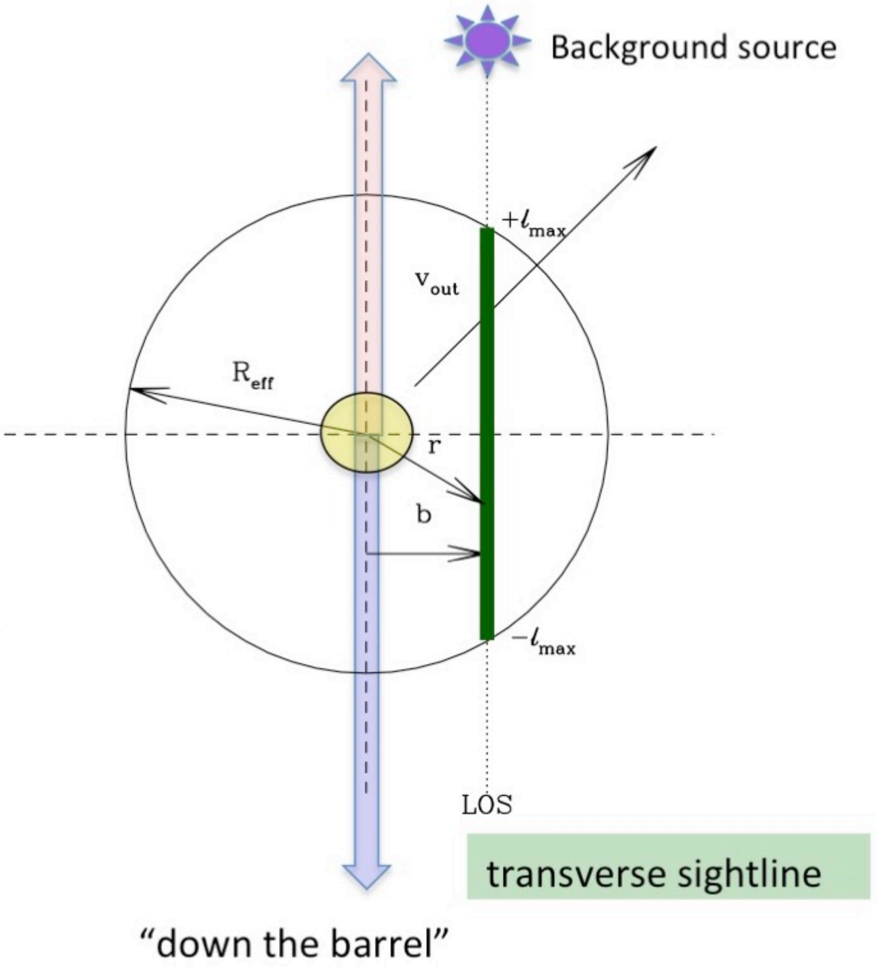

C. Hummels+FIRE team, zoom-in of MW-progenitor $M_{\mathrm{h}} \simeq 10^{12} M_\odot$ at z = 0

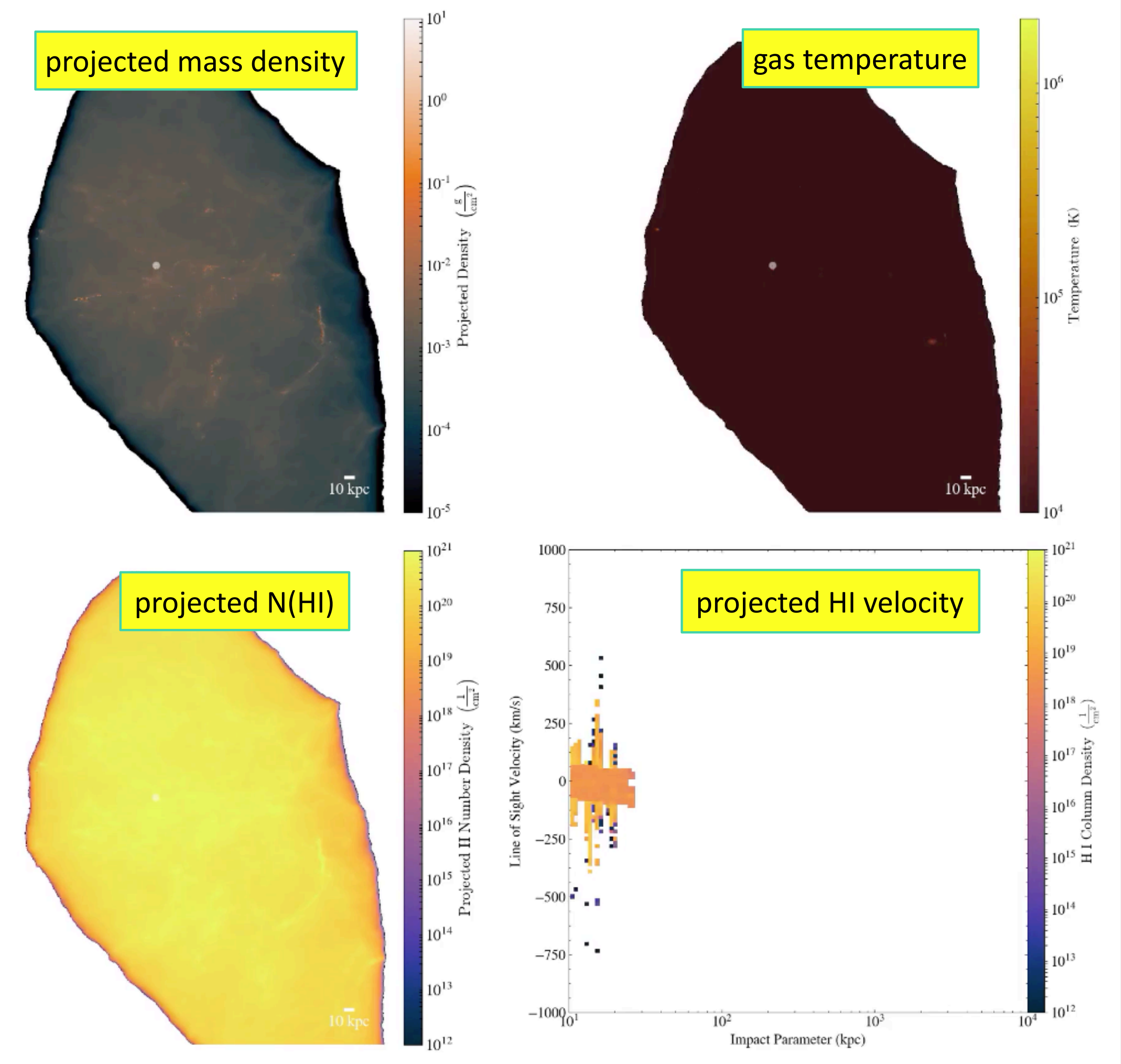

Densely Sampling the Universe @z~1.8-3.5:

“Hi-Fi” Version

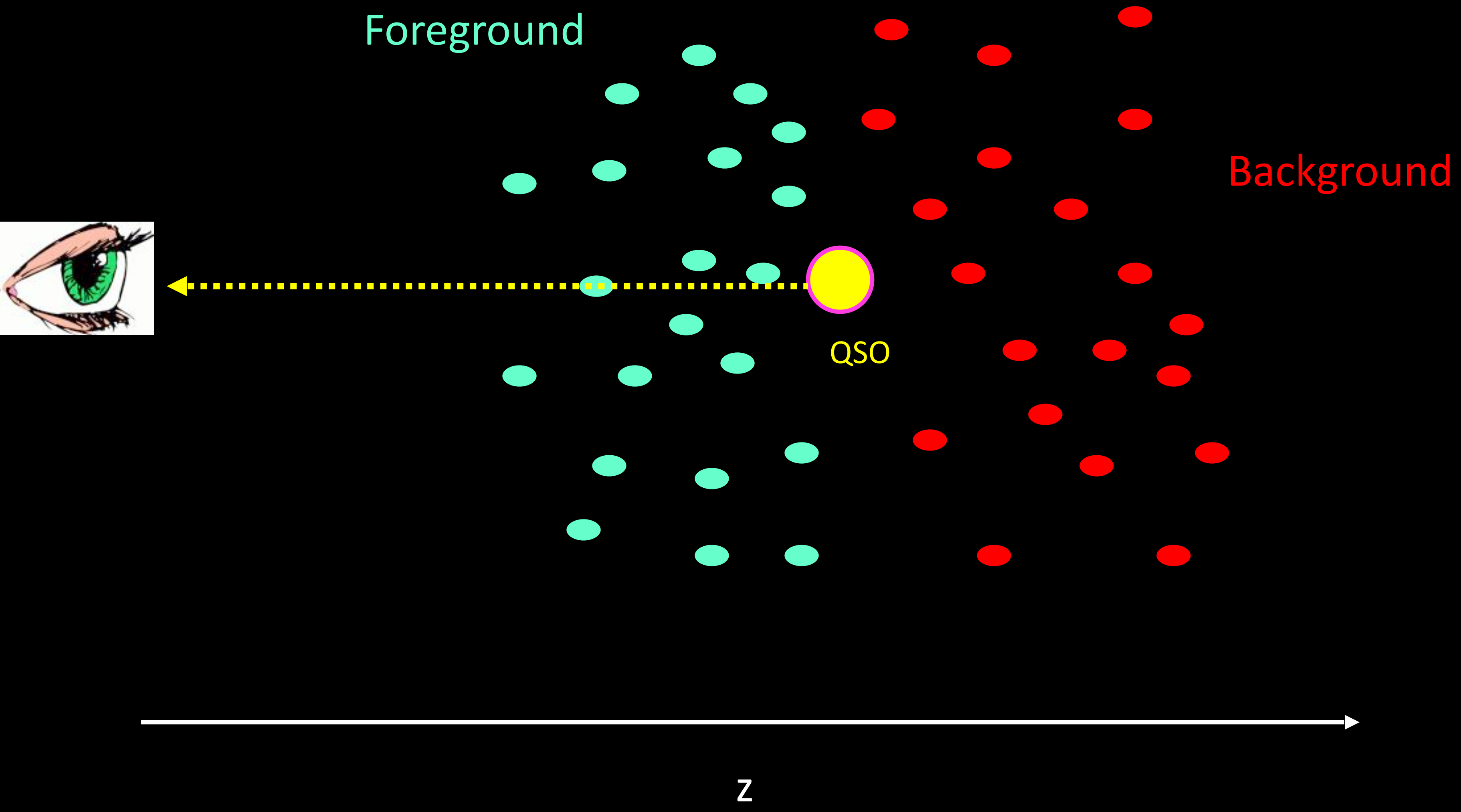

Foreground

Background

QSO

z

Densely Sampling the Universe @z~1.8-3.2

Learning to love the "Lo-fi grid"

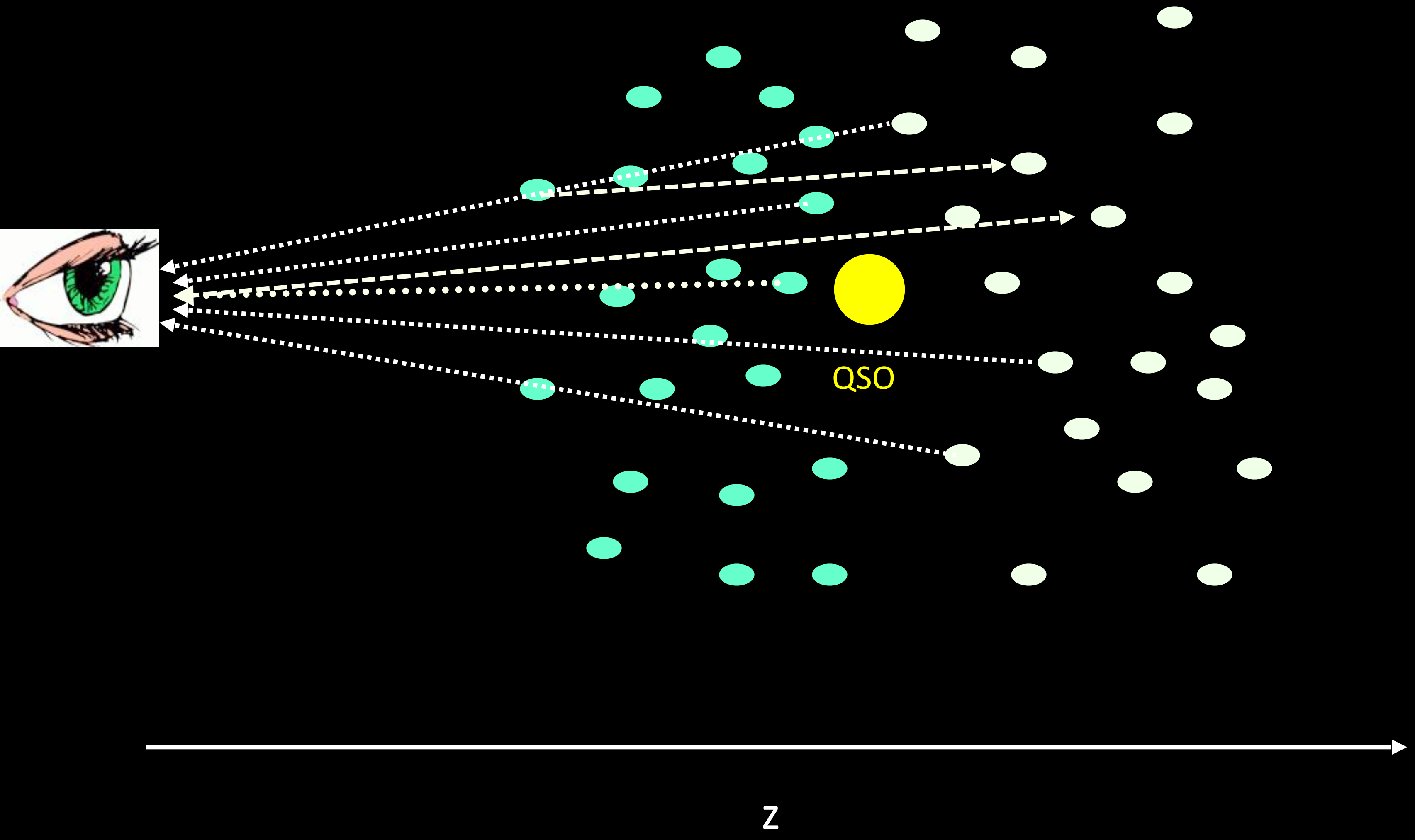

Typical Field, 5.5’ x 7’, 184 spectroscopic redshifts , z~1.5-3.5

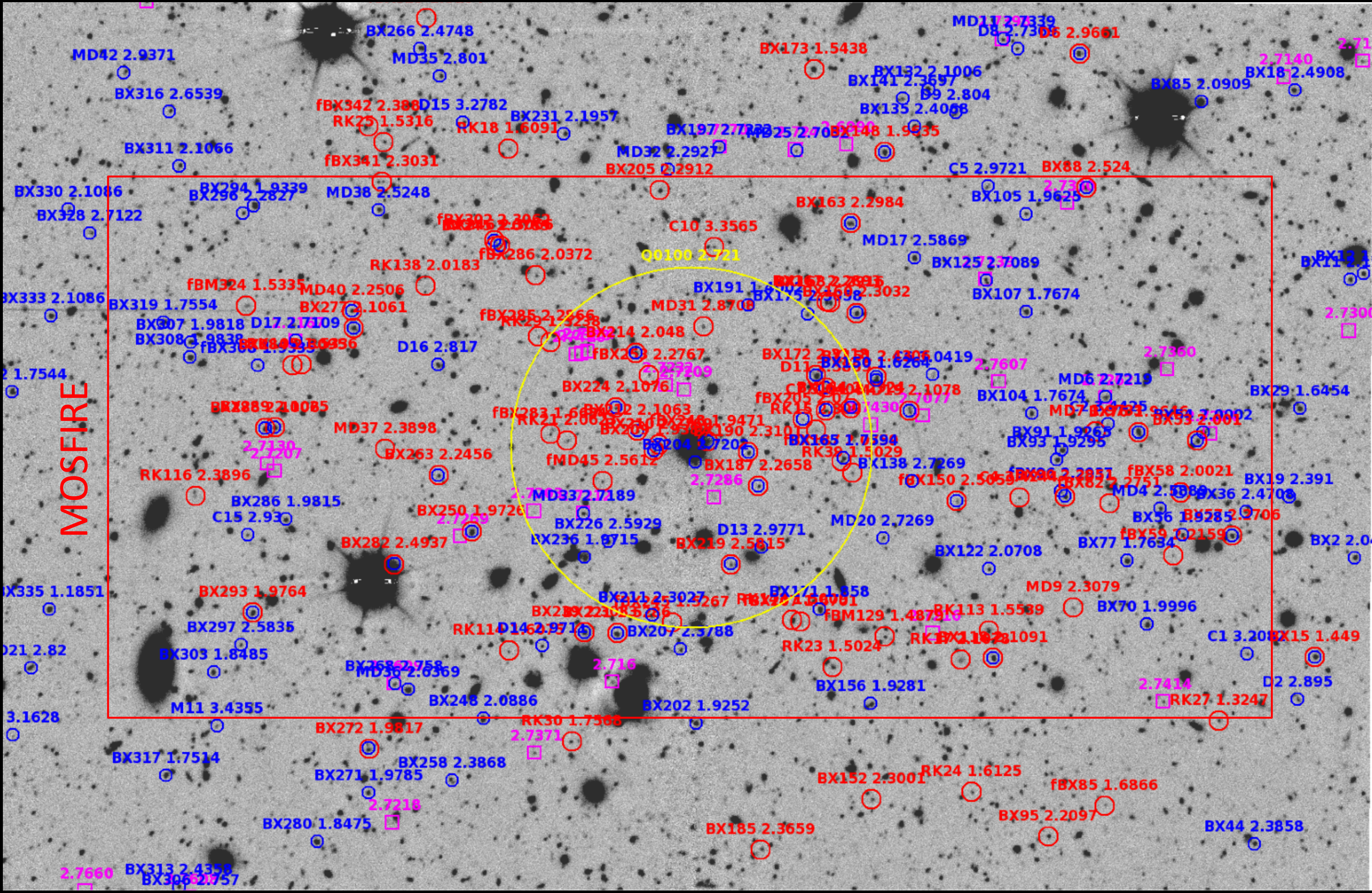

KBSS 0100+13 z_Q=2.721

Lyα absorption halos around z~2 star-forming galaxies

>100,000 foreground/background galaxy pairs <z>=2.2 from KBSS

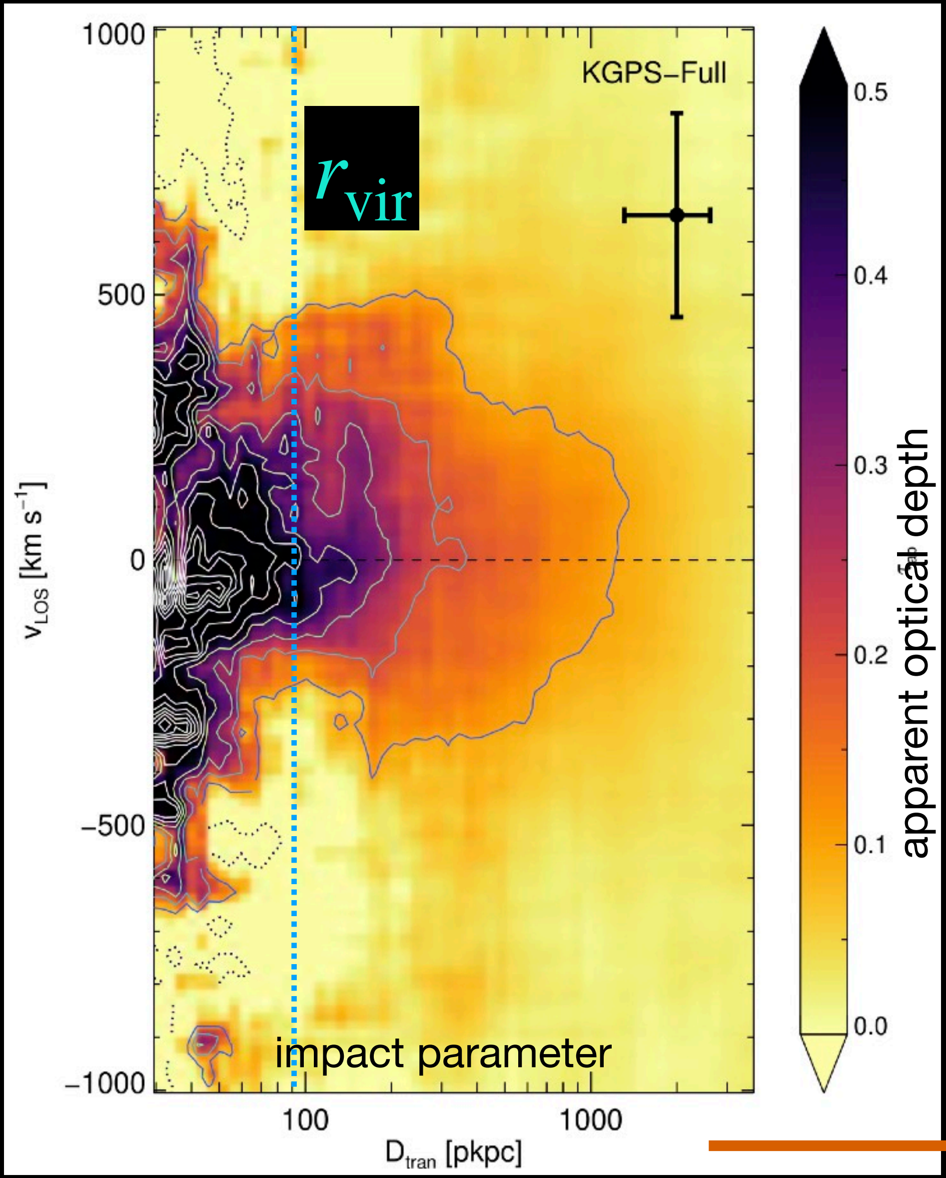

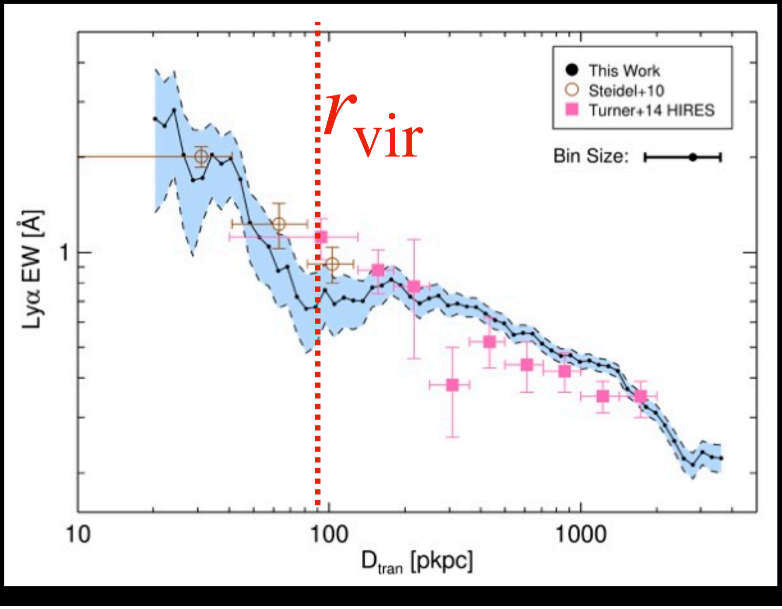

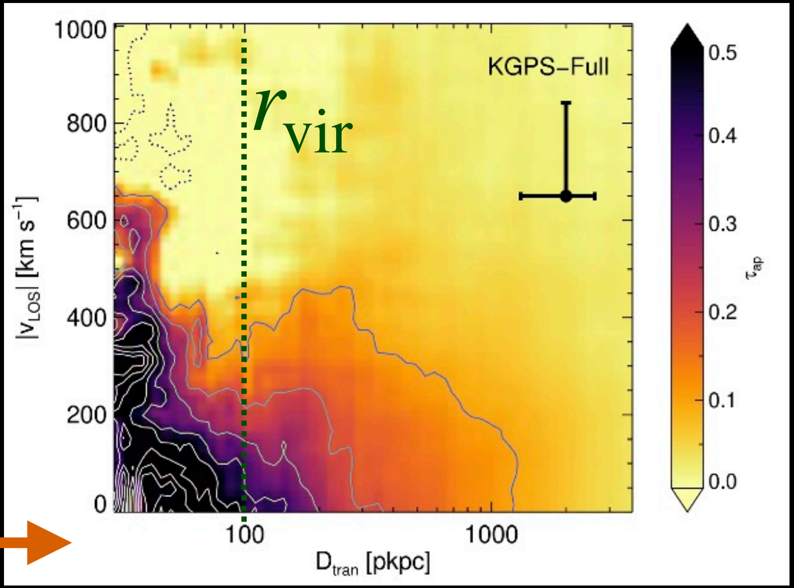

Yuguang Chen, CS, Hummels, Rudie+2019

Galaxy Pair Composite Spectra

50 pairs 1-5” (<d>=30 kpc)

190 pairs 5-10” (<d>=70 kpc)

305 pairs 10-15” (<d>=100 kpc)

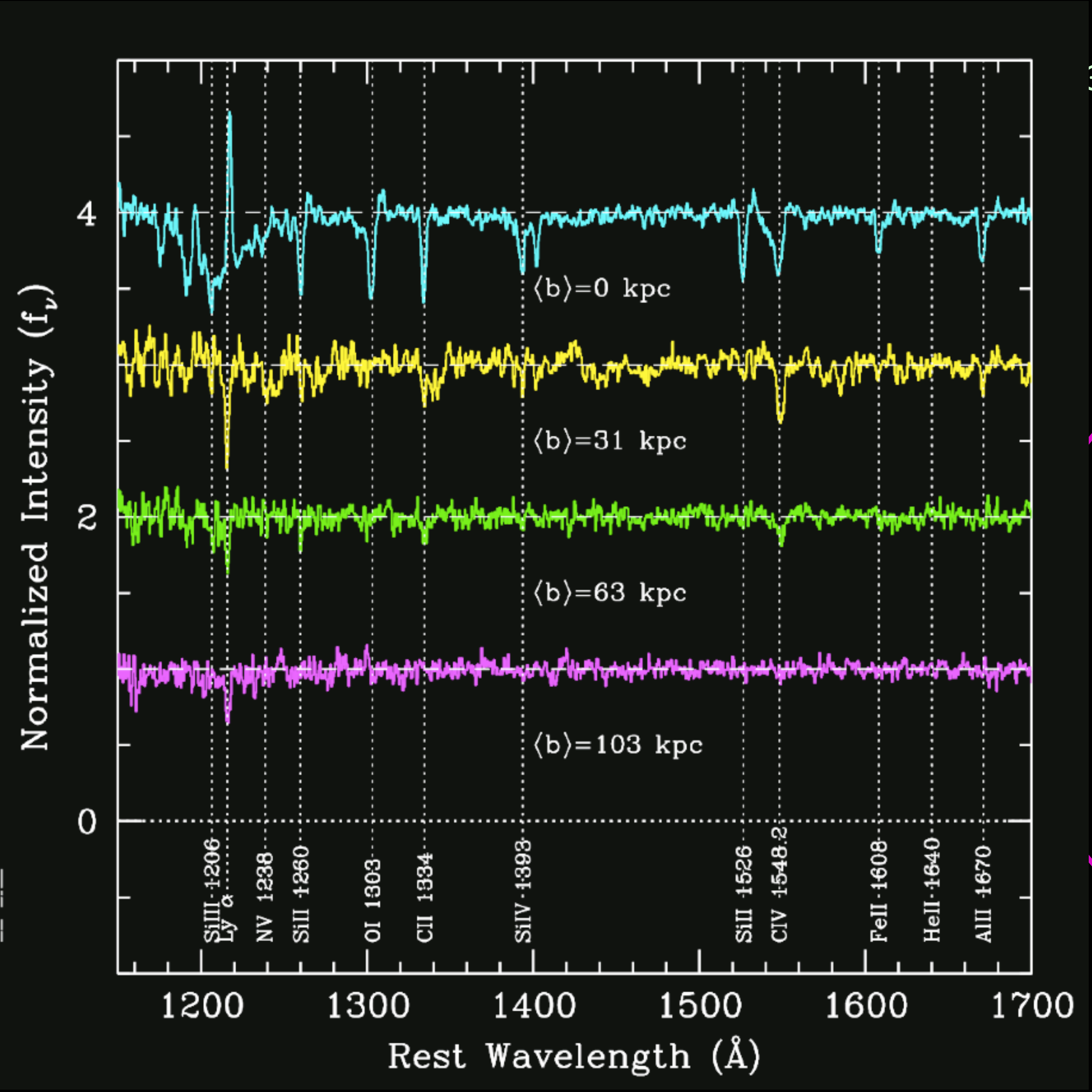

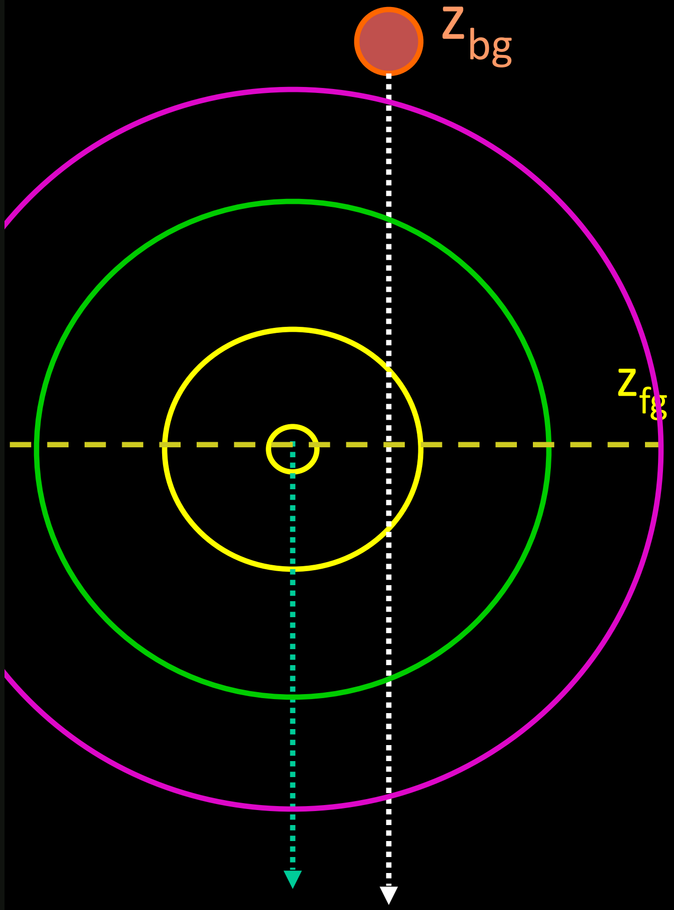

CS+2010

W_0 vs. Galaxy Impact Parameter, z~2-3 LBGs

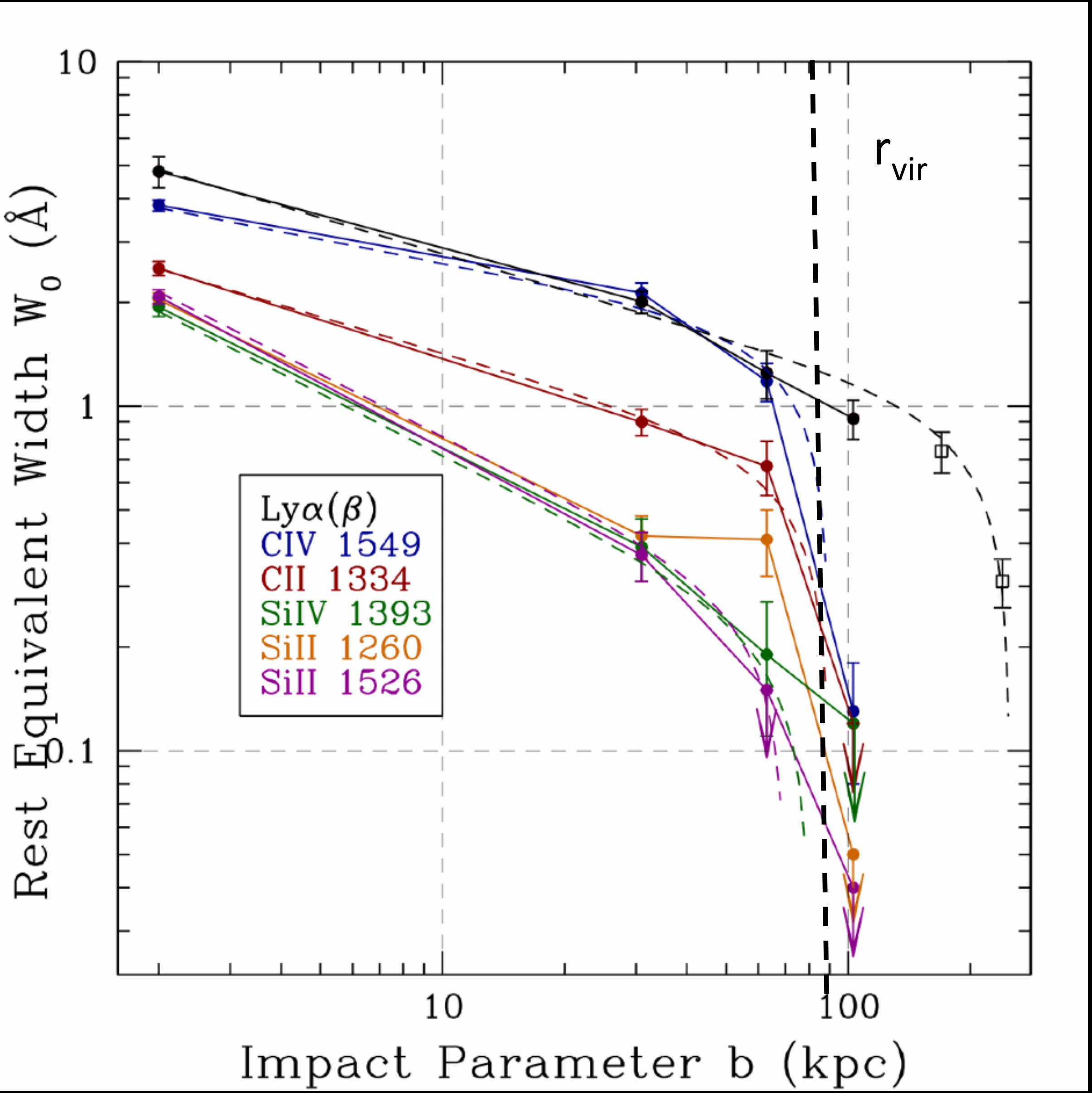

Models:

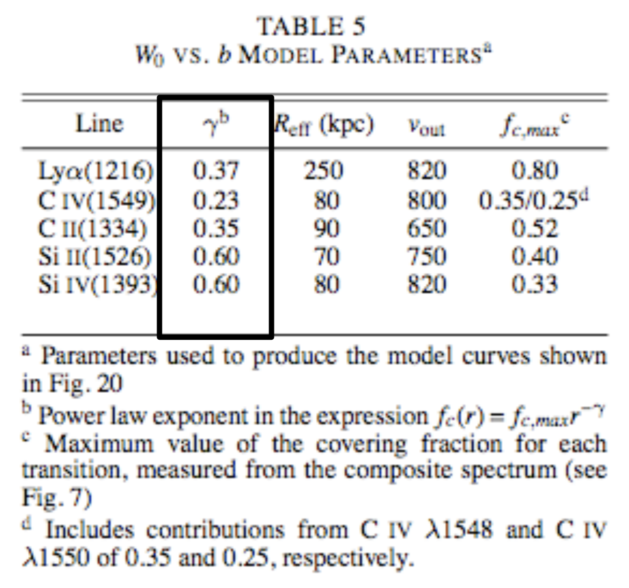

TABLE 5
W_0 VS. b MODEL PARAMETERS[a]

Line	γ[b]	$R_{\rm eff}$ (kpc)	$v_{\rm out}$	$f_{c,max}$[c]
Lyα(1216)	0.37	250	820	0.80
C IV(1549)	0.23	80	800	0.35/0.25[d]
C II(1334)	0.35	90	650	0.52
Si II(1526)	0.60	70	750	0.40
Si IV(1393)	0.60	80	820	0.33

[a] Parameters used to produce the model curves shown in Fig. 20

[b] Power law exponent in the expression $f_c(r) = f_{c,max} r^{-\gamma}$

[c] Maximum value of the covering fraction for each transition, measured from the composite spectrum (see Fig. 7)

[d] Includes contributions from C IV λ1548 and C IV λ1550 of 0.35 and 0.25, respectively.

$f_c(r) \sim r^{-\gamma}$

CS +2010

GOAL: the primordial dark matter power spectrum

CMB physics
z = 1100
dynamics

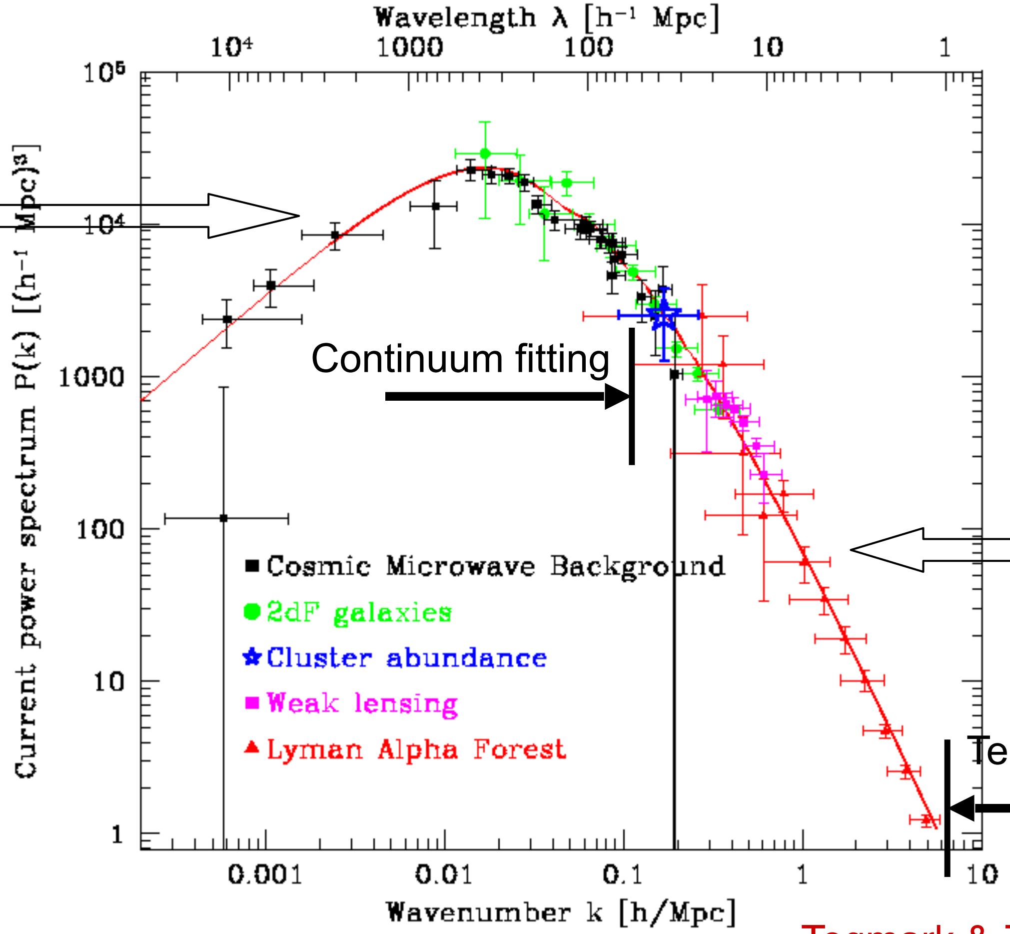

Continuum fitting

Lya physics
z < 6
dynamics
+
thermodynamics

Temperature, metals, noise

Tegmark & Zaldarriaga 2002

Why the Lyman alpha forest? Very small matter over-densities and absence of complicated baryon physics...

REIONIZATION OF THE UNIVERSE

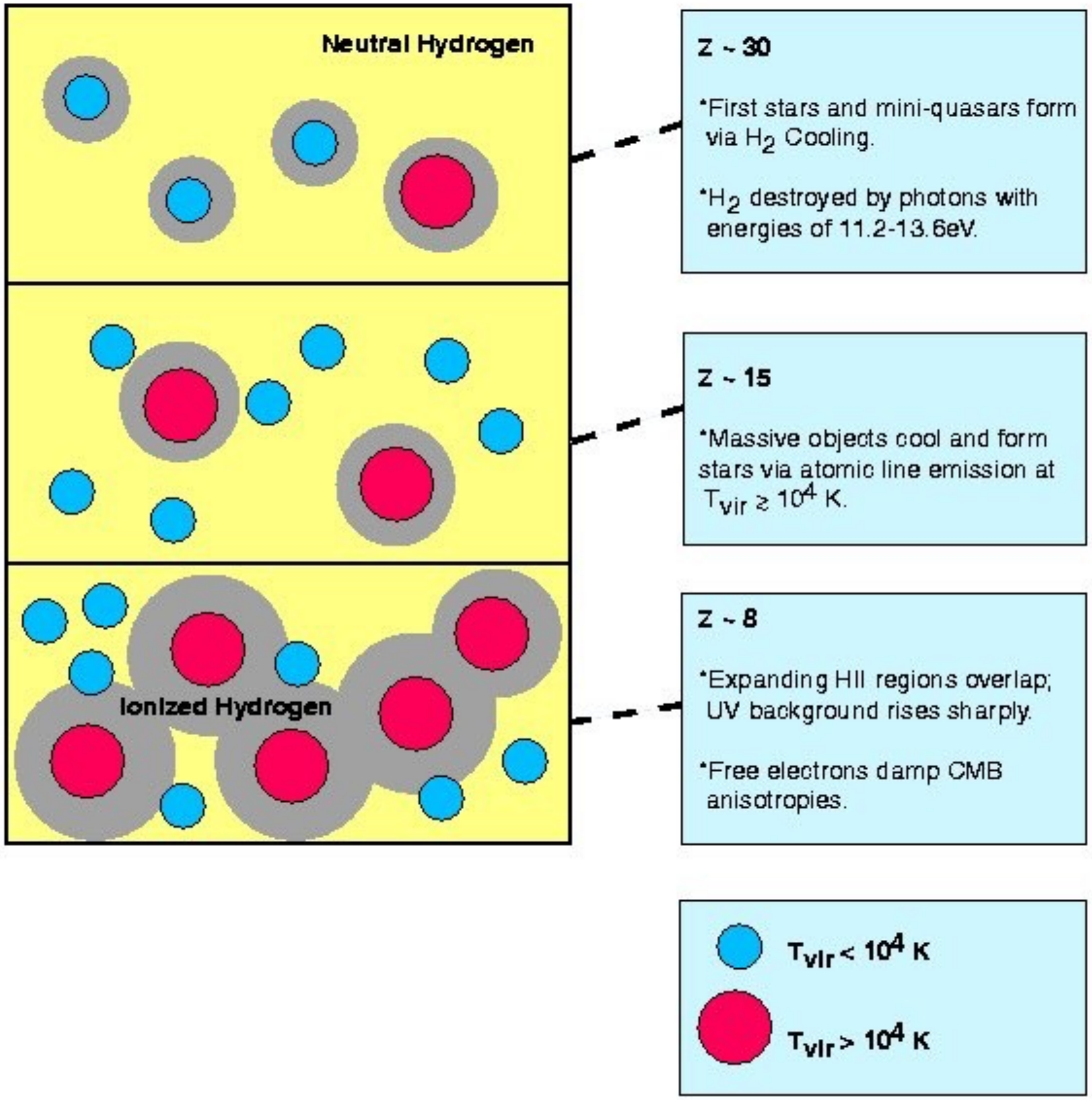

Z ~ 30

- First stars and mini-quasars form via H_2 Cooling.
- H_2 destroyed by photons with energies of 11.2-13.6eV.

Z ~ 15

- Massive objects cool and form stars via atomic line emission at $T_{vir} \gtrsim 10^4$ K.

Z ~ 8

- Expanding HII regions overlap; UV background rises sharply.
- Free electrons damp CMB anisotropies.

From Haiman & Loeb

Three stages

Pre-overlap

↓

Overlap

↓

Post-overlap

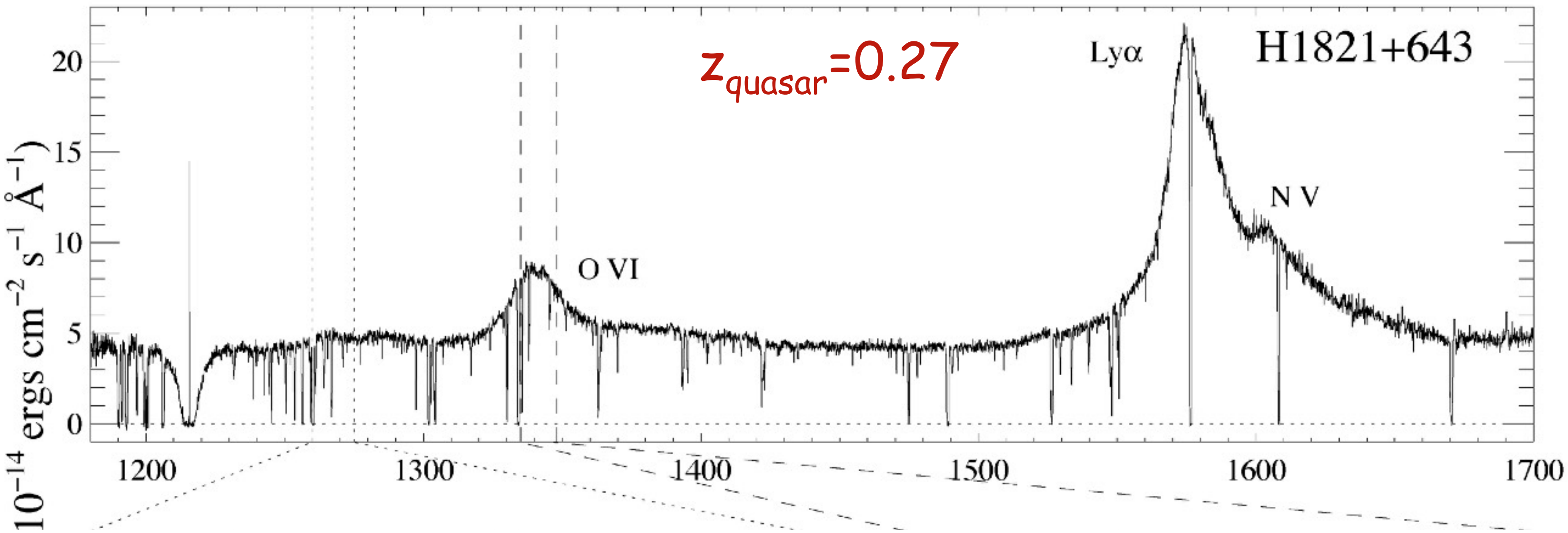

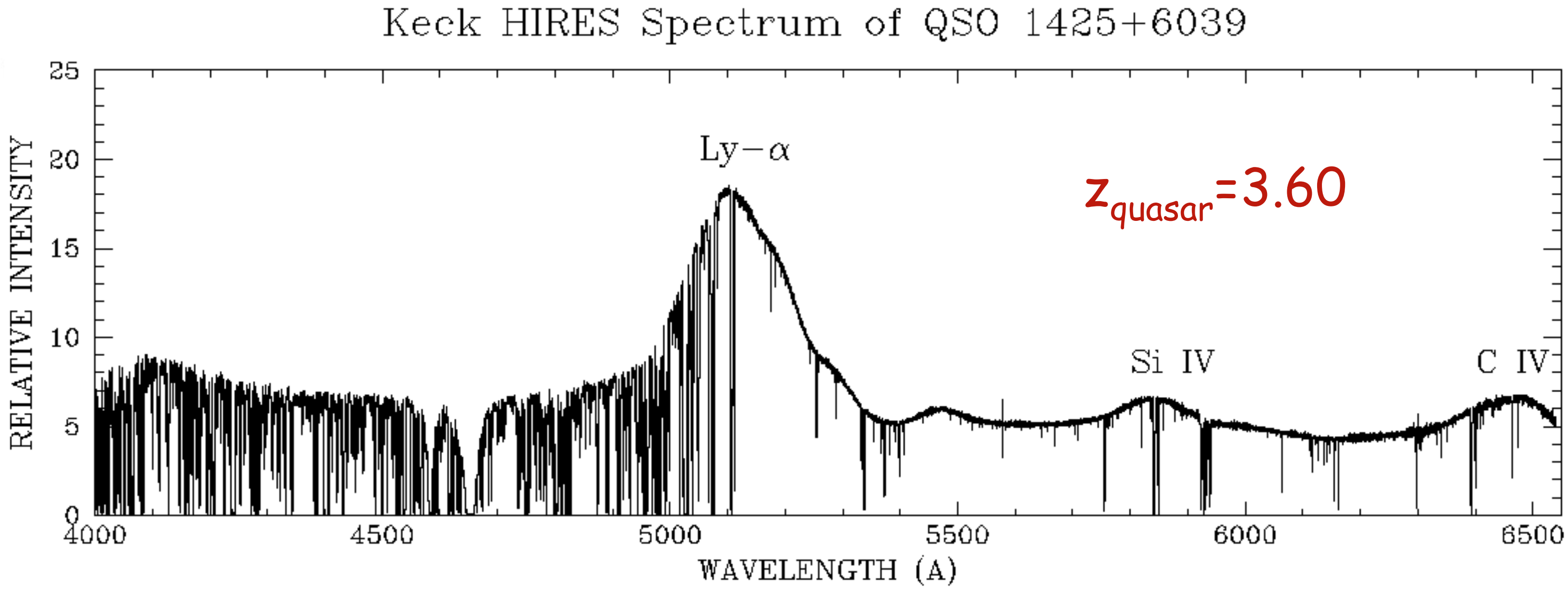

$\lambda_{obs(Lya)}=(1+z_{cloud})\times1216$ Angstroms

In the very highest redshift quasars, the “forest” is so thick that it begins to look like a completely absorbed medium.

Some evidence that at z~6, the intergalactic medium is rapidly becoming entirely neutral.

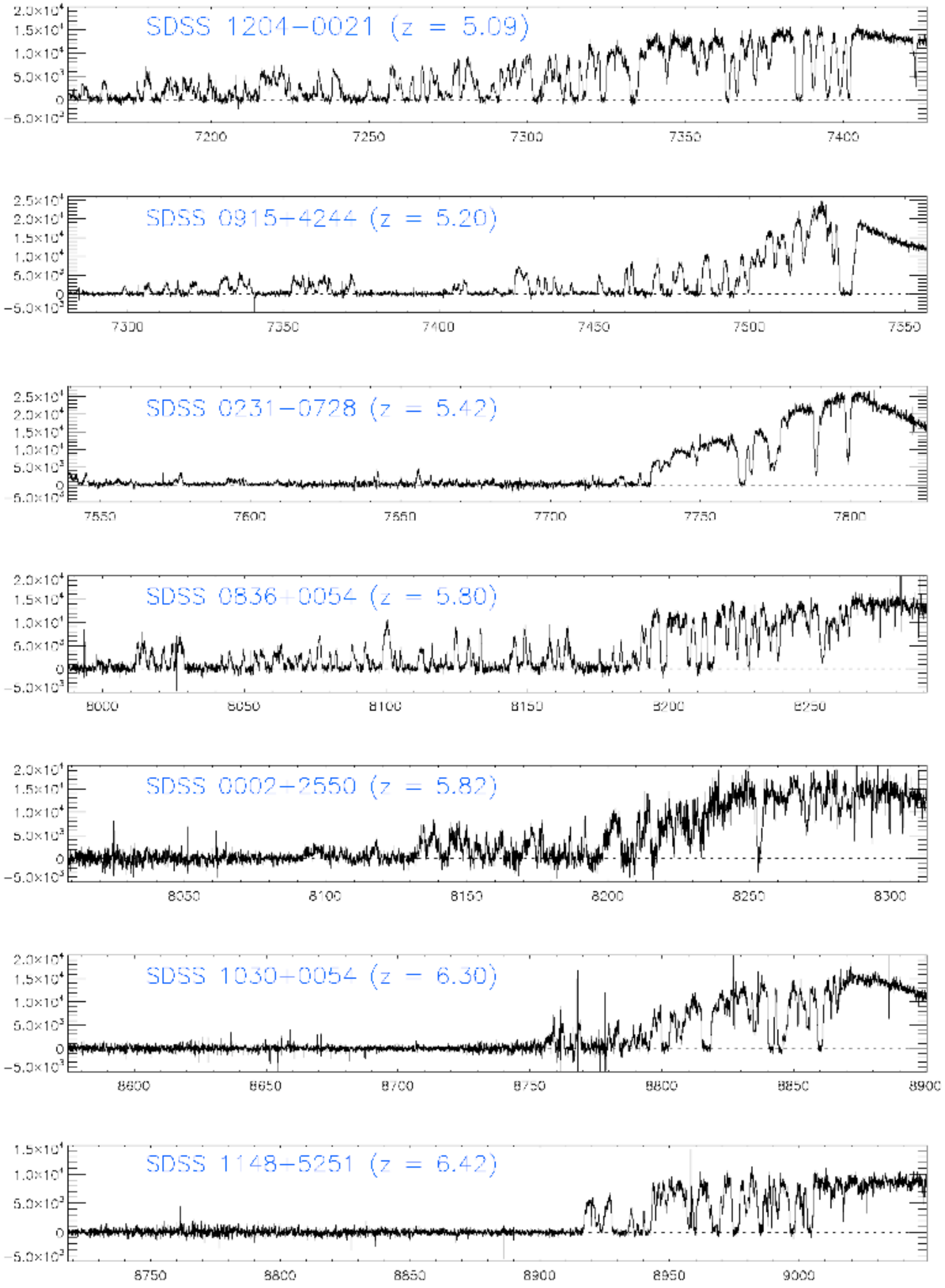

IGM Lyman alpha “Troughs” in the Highest-redshift Quasars

- only ~20 such QSOs in the entire sky! (these are from the Sloan Digital Sky Survey)
- on-set of complete absorption by the IGM at z>5.8?
- is the the “end of the re-ionization era”?

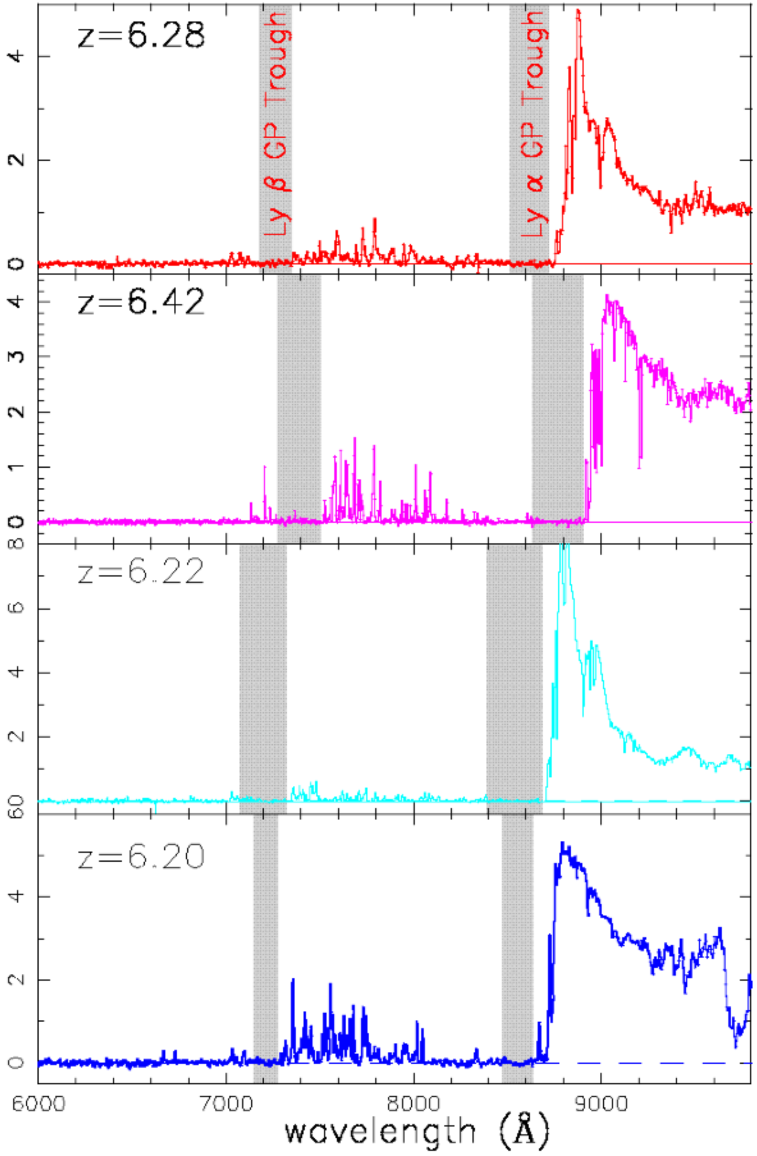

Star Formation/Black Hole Accretion History of the Universe

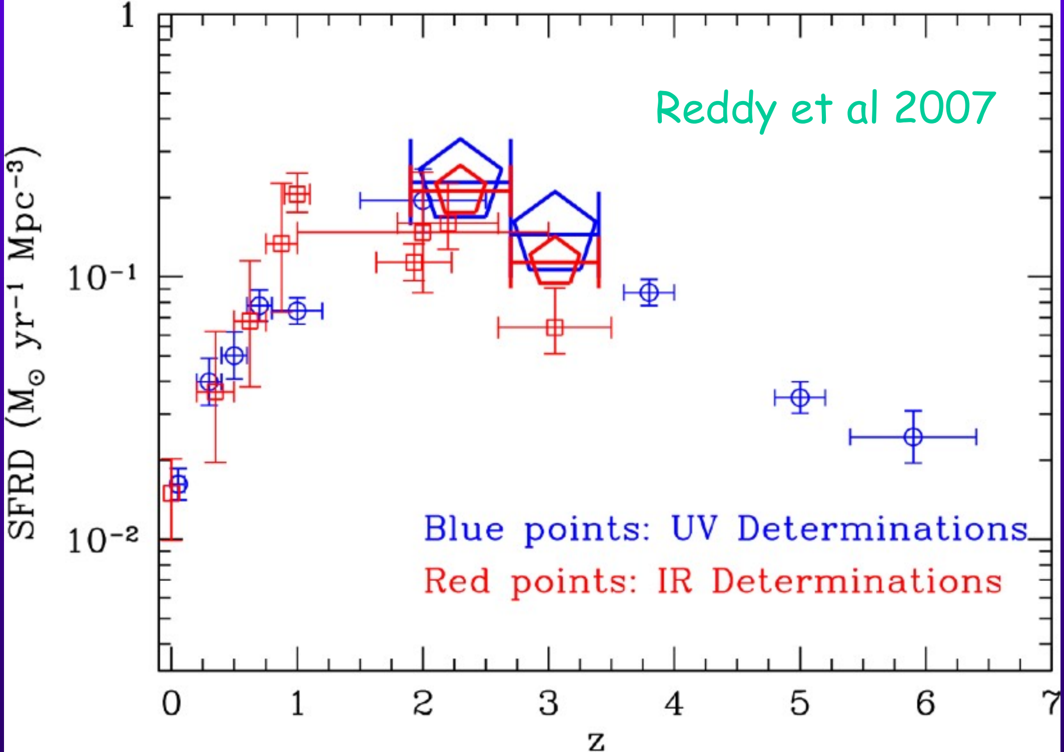

Reddy et al 2007

Galaxies

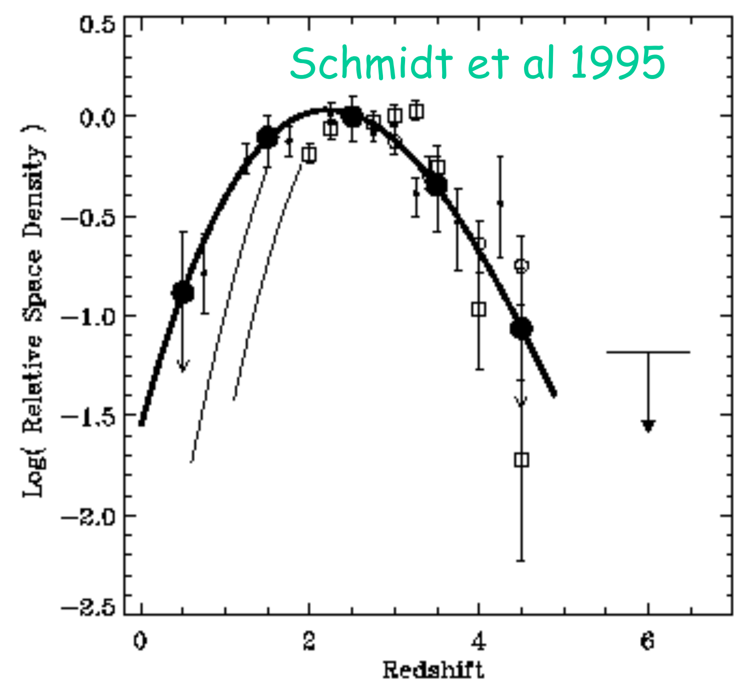

Schmidt et al 1995

Bright Quasars

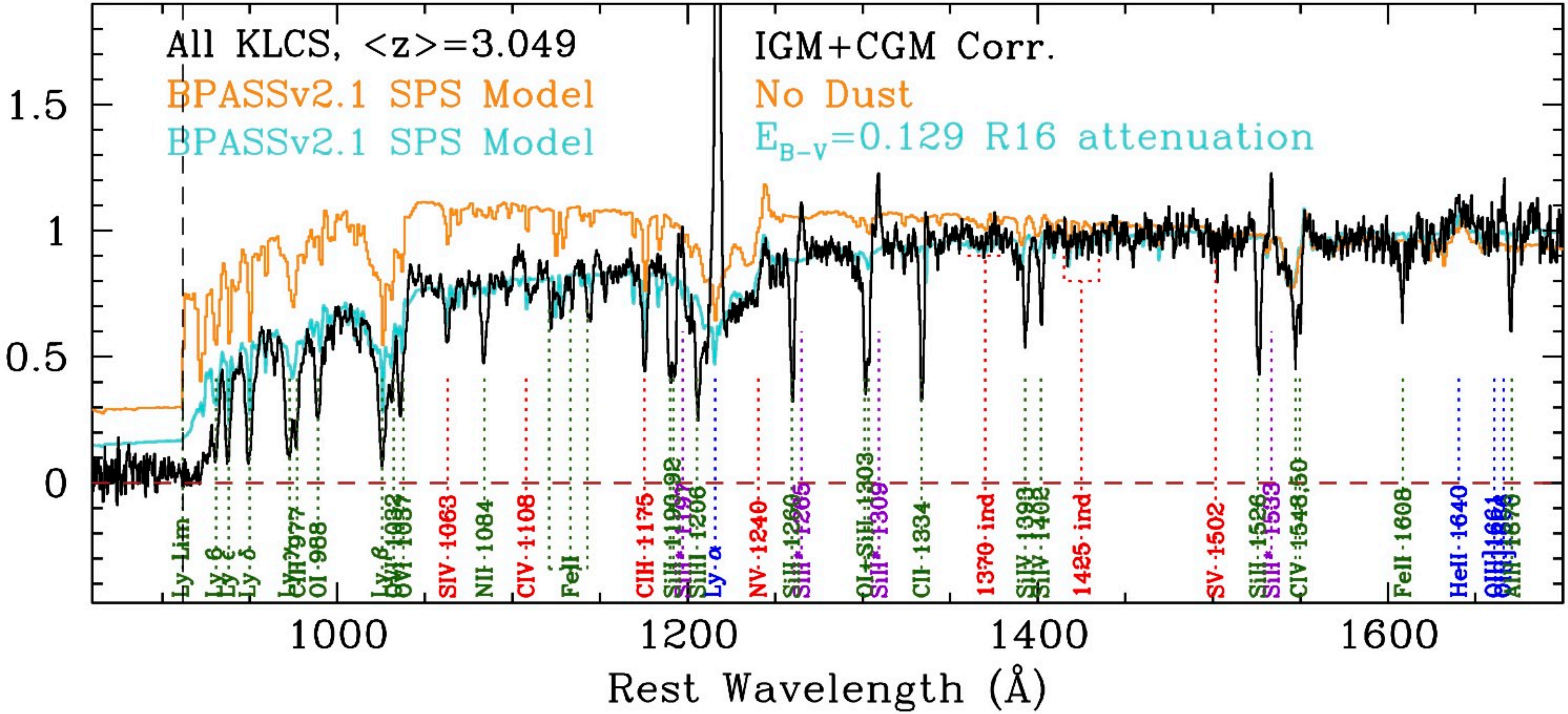All KLCS, <z>=3.049
BPASSv2.1 SPS Model
BPASSv2.1 SPS Model
IGM+CGM Corr.
No Dust
E$_{B-V}$=0.129 R16 attenuation
1.5
1
0.5
0
1000
1200
1400
1600
Rest Wavelength (Å)
Ly Lim
Ly 6
Ly ε
Ly δ
Ly γ
CIII 977
OI 988
Ly β
OVI 1032
OVI 1037
SIV 1063
NII 1084
CIV 1108
FeII
CIII 1175
SiII 1190,92
SiII* 1197
SiIII 1206
Ly α
NV 1240
SiII 1260
SiII* 1265
OI+SiII 1303
SiII* 1309
CII 1334
1370 ind
SiIV 1393
SiIV 1402
1425 ind
SV 1502
SiII 1526
SiII* 1533
CIV 1548,50
FeII 1608
HeII 1640
OIII] 1661
OIII] 1666
AlII 1670

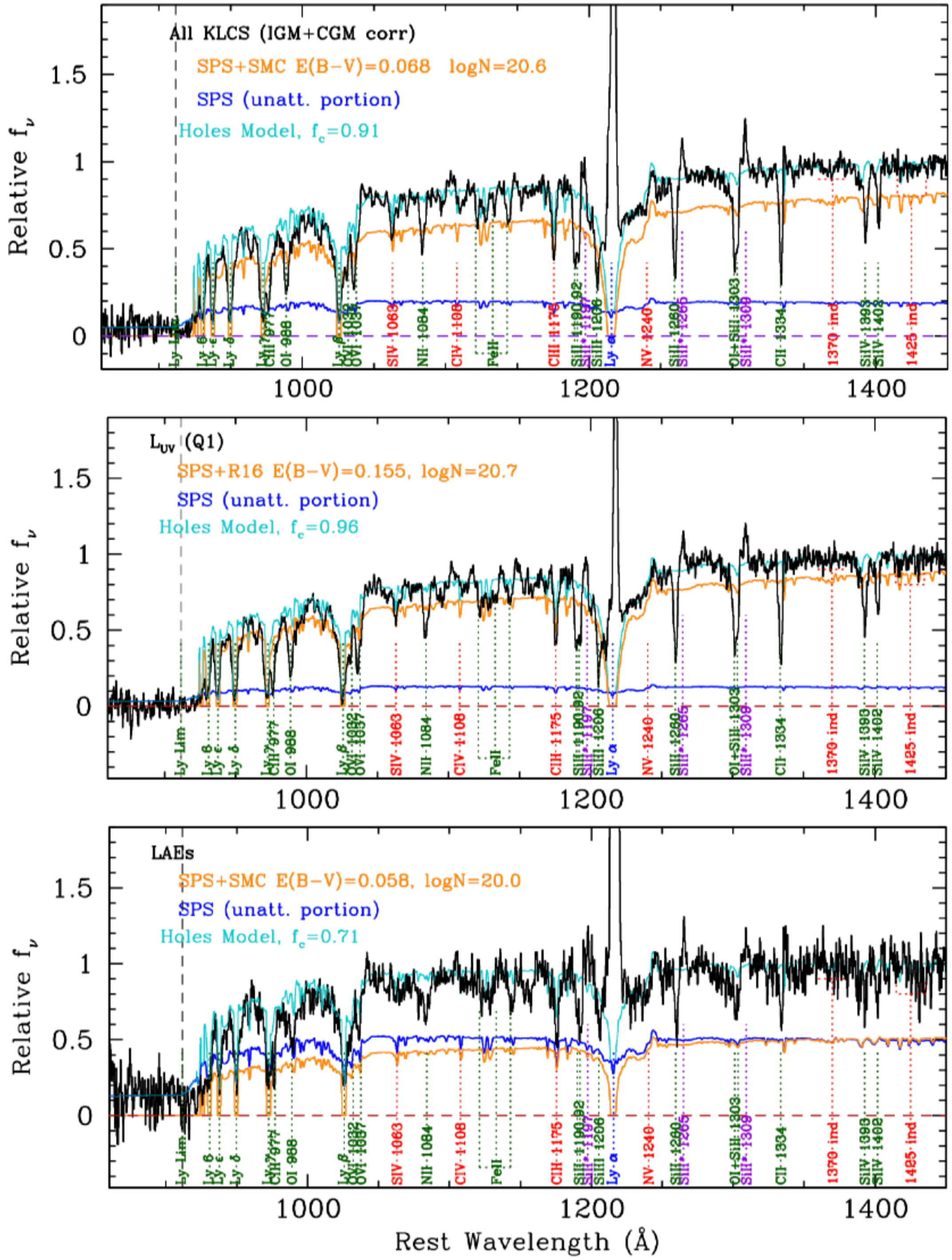

CS+2018

All <z>=3 LBGs

f_{900}/f_{1500} = 0.057±0.006

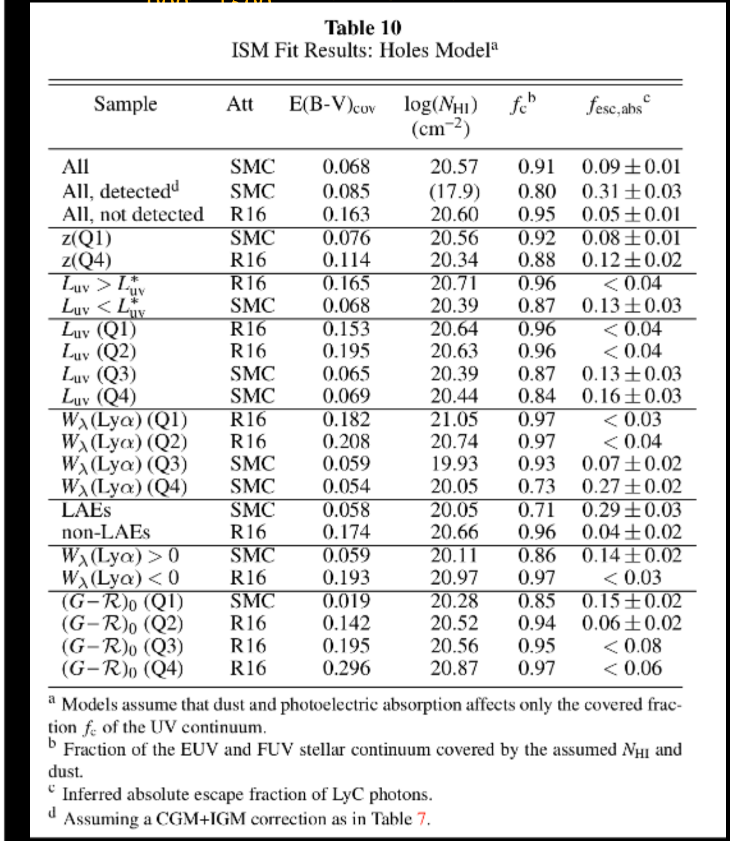

Table 10
ISM Fit Results: Holes Model[a]

Sample	Att	$E(B-V)_{\rm cov}$	$\log(N_{\rm HI})$ ($\rm cm^{-2}$)	f_c[b]	$f_{\rm esc,abs}$[c]
All	SMC	0.068	20.57	0.91	0.09 ± 0.01
All, detected[d]	SMC	0.085	(17.9)	0.80	0.31 ± 0.03
All, not detected	R16	0.163	20.60	0.95	0.05 ± 0.01
z(Q1)	SMC	0.076	20.56	0.92	0.08 ± 0.01
z(Q4)	R16	0.114	20.34	0.88	0.12 ± 0.02
$L_{\rm uv} > L^*_{\rm uv}$	R16	0.165	20.71	0.96	< 0.04
$L_{\rm uv} < L^*_{\rm uv}$	SMC	0.068	20.39	0.87	0.13 ± 0.03
$L_{\rm uv}$ (Q1)	R16	0.153	20.64	0.96	< 0.04
$L_{\rm uv}$ (Q2)	R16	0.195	20.63	0.96	< 0.04
$L_{\rm uv}$ (Q3)	SMC	0.065	20.39	0.87	0.13 ± 0.03
$L_{\rm uv}$ (Q4)	SMC	0.069	20.44	0.84	0.16 ± 0.03
$W_\lambda({\rm Ly}\alpha)$ (Q1)	R16	0.182	21.05	0.97	< 0.03
$W_\lambda({\rm Ly}\alpha)$ (Q2)	R16	0.208	20.74	0.97	< 0.04
$W_\lambda({\rm Ly}\alpha)$ (Q3)	SMC	0.059	19.93	0.93	0.07 ± 0.02
$W_\lambda({\rm Ly}\alpha)$ (Q4)	SMC	0.054	20.05	0.73	0.27 ± 0.02
LAEs	SMC	0.058	20.05	0.71	0.29 ± 0.03
non-LAEs	R16	0.174	20.66	0.96	0.04 ± 0.02
$W_\lambda({\rm Ly}\alpha) > 0$	SMC	0.059	20.11	0.86	0.14 ± 0.02
$W_\lambda({\rm Ly}\alpha) < 0$	R16	0.193	20.97	0.97	< 0.03
$(G-\mathcal{R})_0$ (Q1)	SMC	0.019	20.28	0.85	0.15 ± 0.02
$(G-\mathcal{R})_0$ (Q2)	R16	0.142	20.52	0.94	0.06 ± 0.02
$(G-\mathcal{R})_0$ (Q3)	R16	0.195	20.56	0.95	< 0.08
$(G-\mathcal{R})_0$ (Q4)	R16	0.296	20.87	0.97	< 0.06

[a] Models assume that dust and photoelectric absorption affects only the covered fraction f_c of the UV continuum.
[b] Fraction of the EUV and FUV stellar continuum covered by the assumed $N_{\rm HI}$ and dust.
[c] Inferred absolute escape fraction of LyC photons.
[d] Assuming a CGM+IGM correction as in Table 7.

W(Lyα) > 20 Å (LAEs)

f_{900}/f_{1500}= 0.175±0.026

$f_{\rm esc,abs}$=0.29±0.03